International Journal of

Young Scientist Research
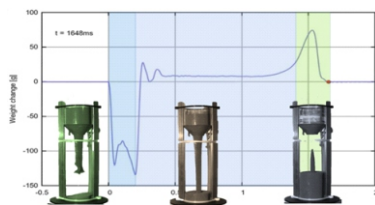
Contents

Young Scientist Research

Young Scientist Research is a research journal based on scientific projects . This open-access journal includes young students' research in any field of science which publishes full-length and abstract research on any aspects of applied sciences in relation to work presented in both national and international conferences, competitions and tournaments of all types. New manuscripts sent to the Journal will be handled by the Editorial Office who checks compliance with the guidelines to authors. Then a rapid screening process at which stage a decision to reject or to go to full review is made.

By submission of a manuscript to the Journal, all authors warrant that they have the authority to publish the material and that the paper, or one substantially the same, has neither been published previously, nor is being considered for publication elsewhere.

This journal belongs to Ariaian Young Innovative Minds Institute, AYIMI, and one to two issues is published in a year. All details are on the http://iypt.ir website.

CORROSION PROTECTION IN A SPECIFIC KIND OF AL ALLOY IN MARINE ENVIRONMENT

D. Izadi [a] , M.Torabi.Azad [b]

a) Ariaian Young Innovative Minds Institute, Tehran, Iran, info@ayimi.org
b) Islamic Azad University, Tehran North Branch,Tehran, Iran, torabi_us@yahoo.com

ABSTRACT

Compared to iron and steel, aluminum alloys have the advantages of lower density, higher specific strength and superior corrosion resistance. Therefore, lightweight aluminum alloys are being considered for use in aircraft, automobiles, railroad cars, and ships. In this study we are going to protect a specific Aluminum alloy which is used in marine industries such as submarines against corrosion. Thus, early studies on the corrosion behaviour of this alloy in two different seawater solutions (x, y) was carried out to find how to protect it according to the results of previous studies conducted by researchers. Pitting is the main part of the corrosion of this alloy in marine environments and we are going to minimize this type of corrosion.

1 Introduction

Corrosion is one of the biggest maintenance problems in vessels of all sizes, particularly in saltwater. Corrosion above the water line is one thing; your only defence there is frequent inspection and careful attention to painting, cleaning, and greasing. Corrosion of hull fittings and metals below the water line, however, is another matter. It can be controlled by cathodic protection. Adequate protection can be achieved by using either zinc sacrificial anodes or impressed current systems. Corrosion is an electrochemical process in which a chemical reaction takes place, creating a flow of electrical charge, or current, between two unlike metals. This chemical action between two unlike metals can destroy one of the metals. When that metal is a propeller, strut, or shaft, the damage can grow expensive. One cannot understand or design an adequate cathodic protection system without a basic knowledge of direct-current (D.C.) electrical theory. Ohm's Law is a handy starting point: Briefly, it states that current (I) in a circuit is proportional to the potential difference (E) across a circuit. Voltage is often compared to water pressure. Then, the water flowing under pressure through a pipe behaves like electricity. The amount of water moving through the pipe is analogous to the current. The frictional resistance to water flow within the pipe is the counterpart of the electrical resistance. Most of the discussion that follows relates to factors on and around boats in saltwater (and to a less severe extent, to those in freshwater) that can reduce the unwanted current that causes corrosion [1]. Al–Mg alloys are not heat-treated, and show high strength and good welding properties. They are often used in high pressure vessels, ships, and other marine structures because they have good corrosion resistance in seawater environments. In this study to find the corrosion protection in a specific Al alloy the Chemical compounds and elements in this alloy were studied and then by using accepted standards, it was surveyed.

2. Materials and Methods

In the beginning by using emission spectrometry the chemical compounds and elements in the alloy were studied and then by using accepted standards, it was surveyed. The results of the analysis Quantometre are given in table (1). As shown the main elements in this alloy are Al and Mg which according to the standards of Al alloy, this is very near to AA5083. The percentage of this composition is given in table (2)[2].

Table 1: Chemical composition of the sample in elements weight percentage

Si	Fe	Cu	Mn	Mg	Cr	Ni	Zn	Ti	Be	Ca	Li
0.10	0.20	0.05	0.60	4.9	0.09	0.004	0.02	0.01	Trace	Trace	Trace
Pb	Sn	Sr	V	Na	Bi	Co	Zr	B	Ga	Cd	Al
Trace	< 0.005	Trace	0.01	Trace	< 0.004	0.003	Trace	0.002	0.01	0.002	Base

Table 2: Standard chemical composition of the alloy

	Si	Fe	Cu	Mn	Mg	Cr	Zn	Ti	Other each	Other total	Al
Min	*	*	*	0.40	4.0	0.05	*	*	*	*	Rem
Max	0.40	0.40	0.10	1.0	4.9	0.25	0.25	0.15	0.05	0.15	*

Before testing 5083 alloy it is necessary to study the properties of this alloy and its corrosion behaviour in several environments especially in marine environments.

2-1 Physical Properties of alloy 5083

Aa5083 Al- Mg alloys for high corrosion resistance, low density and good mechanical properties are widely used in the marine industry to manufacture vessels and submarines [3, 4]. Mechanical properties of these alloys are given in table (3).

Table 3: Mechanical properties of AA5083 alloys

Physical Properties	Metric	English
Density	2.66 g/cc	0.0961 lb/in³
Mechanical Properties		
Hardness, Brinell	85	85
Hardness, Knoop	109	109
Hardness, Rockwell A	36.5	36.5
Hardness, Rockwell B	53	53
Hardness, Vickers	96	96
Ultimate Tensile Strength	317 MPa	46000 psi
Tensile Yield Strength	228 MPa	33000 psi
Elongation at Break	16 %	16 %
Modulus of Elasticity	70.3 GPa	10200 ksi
Modulus of Elasticity	71 GPa	10300 ksi
Compressive Modulus	71.7 GPa	10400 ksi
Poisson's Ratio	0.33	0.33
Fatigue Strength	159 MPa	23000 psi
Fracture Toughness	43 MPa-m½	39.1 ksi-in½
Machinability	30 %	30 %
Shear Modulus	26.4 GPa	3830 ksi
Shear Strength	190 MPa	27600 psi

These alloys owe their strength to intermetallic compounds. But the existence of this particular type of compound will cause corrosion so that by oxygen reduction on the intermetallic compounds and based on the following equation the hydroxide ion will be generated and as a result the environment of metal compounds changes to alkaline [5,6].

$$H_2O + 1/2O_2 + 2e \leftrightarrow 2OH^{-1} \qquad (1)$$
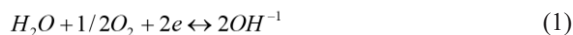
10 years studies on different kinds of Al alloys in sea water and the depth of corrosion show that 5083 Alloy is more resistant against corrosion (table 4).

Table 4: Aluminum alloys Corrosion in seawater after 10 years

Alloy (Russian analog)	The maximum pit depth, mm		
	Harbor island (North Carolina)	Halifax (Nova Scotia)	Ixvimolt (British Columbia)
1100–H14 (АДН)	1.02	0.81	0.76
3003–H14 (АМпH)	0.53	0.56	0.51
5052 (AMr2)	0.10	0.30	0.40
5083 (AMr4)	0.25	0.36	0.45
5056 (AMr5)	0.44	0.49	0.57
6061–T4 (АД33Т)	0.36	0.84	1.27
6061–T6 (АД33Т1)	2.41	1.37	2.95
7072 (АЦпл)	1.42	3.81	0.66
7075T6 (В95Т1)	1.68	(through)	(through)*

* The specimen thickness was 6.4 mm.

3 Experimental Observations

Aluminium alloy sample was cut to dimensions $1 \times 1\ cm$ and then was mounted by particular resin polystyrene in specific frames. So as to leave an exposed area was polished with (400-2500) emery paper. Each specimen was first put in acetone for 5 min. and then in (200) KOH and HNO_3 50% during 30 s and then washed completely by distilled water. According to the previous studies the specimen was put in two different $g \cdot L^{-1}$ seawater solutions (x, y) about 10 hours. First, to check the quality of corrosion rate, ectrochemical impedance tested (EIS) 5083 alloy in both the open circuit potential of the sample dissolved in a solution of x and y respectively.

Electrochemical techniques of corrosion measurement are currently experiencing increasing popularity among corrosion engineers, due primarily to the rapidity with which these measurements can be made. Long term corrosion studies, such as weight loss determinations, may take days or weeks to complete, while an electrochemical experiment will require, at most, several hours. The speed of electrochemical measurements is especially useful for those metals or alloys that are highly corrosion resistant [7].

As is clear from figures (1) and (2) , the corrosion behaviour of the alloy in the two solutions x and y has not significant difference. It seems that charge transfer resistance in the solution x is greater than y.
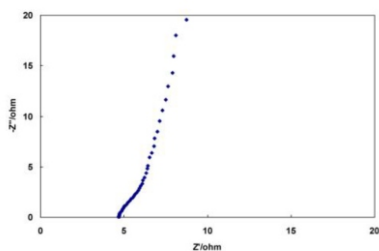

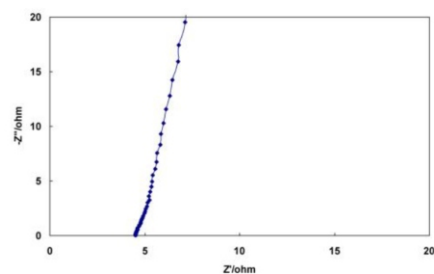Fig.1: Impedance diagram of the specimen alloy in the solution x

Fig. 2: Impedance diagram of the specimen alloy in the solution Y

The next test was Tafel to investigate the corrosion of the 5083 alloy in the range of -2 to 0 V relative to the reference electrode Ag / AgCl, respectively. Tafel plots can provide a direct measure of the corrosion current, which can be related to corrosion rate. The technique is extremely rapid compared to weight loss measurements. The Tafel constants, β_A and β_C, obtained from Tafel plots can be used with Polarization Resistance data to calculate corrosion rates. Tafel analysis is a conventional DC technique in which larger, applied potentials are used. This produce a measurable current which the current-potential is nonlinear and a semi- log plot which is called "Tafel" plot, is used. It shows an Anodic branch for the oxidation reaction and a Cathodic branch for the reduction reaction. The slopes of these two lines (Anodic and Cathodic) are the Tafel coefficients [7,8].

Figures (3) and (4) show Tafel diagram in two solutions x and y. As follows from the figure, corrosion potential, corrosion current and the slope of the cathodic and anodic corrosion of this specimen in both solutions X and Y are nearly the same as each other. Corrosion current in solution x is rather less than in solution y. However, the similarity of the corrosion current in two solutions will cause the type of corrosion protection in the alloy to be the appropriate one. The higher relative corrosion current in solution y with respect to x may be due to the high pH of the solution y (about 8.5) than the solution x (about 7.5).
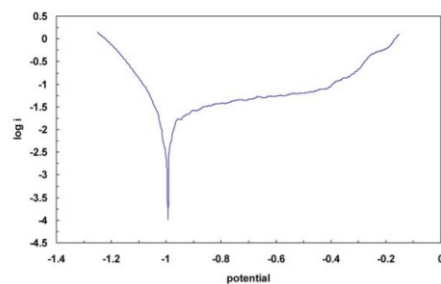

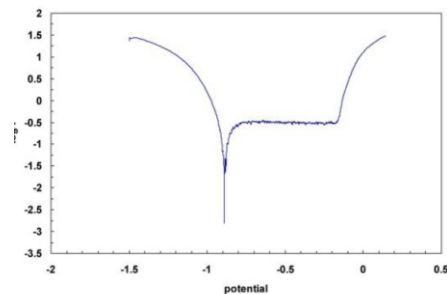Fig. 3 : Tafel diagram of the specimen alloy in the solution x

Fig. 4: Tafel diagram of the specimen alloy in the solution Y

4 Discussion

According to the previous studies and the results of these tests we can come into conclusion that the best way for corrosion protection of this alloy is sacrificial anodes with polymer coatings. Sacrificial anodes for corrosion protection due to the potential difference between the anode and alloy are Zn or Mg anodes.

But the corrosion rate of magnesium in the marine environment is too high, so this type of anode is not affordable. Zn anode is suitable for corrosion protection of the alloy but one of the most important issues is the use of pure Zn metal may cause the Zn to be passivated during the protection and thus loses its protective properties. So to avoid this problem it is necessary to use Zn alloys.

5 Conclusion

Generally, sacrificial anodes used must meet the following conditions:

1-   corrosion potential to be more negative for cathodic polarization structures

2-   uniformly corrosion in environment and stability of the current with the construct under the protection

3-   inactivation of the anode

4-   convenient and cost-effectiveness in terms of electrical capacity

For example, Zn-In sacrificial anodes due to uniform corrosion, make stable potential for cathodic protection relatively so they are profit for environments such as sea water with high corrosion and conductivity. The main factor in steady corrosion of Zn-In alloy in NaCl and seawater environments is its inactivation due to in activating effect in breaking the passive layer.

References

[1]   Mallon M.H., 1979. G Cathodic protection for boats in saltwater , Department of Agricultural Engineering, Oregon State University,
https://ir.library.oregonstate.edu/downloads/5t34sk36j

[2]   Bethencourt M. and Botana F.J. et al., 1998. Material Science Forum, 289-292, pp.567-574.

[3]   Sikora E., Wei X. J. and Shaw B.A., 2004. Corrosion, Vol. 60, No.4, pp.387-394.

[4]   Liu Y., zhou X. , Thompson G.E., Hashimoto T., Scamans G.M. and afseth A. ,2006, Journal of Physics,Vol. 26, pp. 103-106.

[5]   Material and Welding, Vol. 2, p. 79, Korea Register of Shipping (2004).

[6]   Aballe, Bethencourt M. and Botana F.J., 2003. Corrosion Science, Vol. 45, pp.161-180.

[7]   Basics of Corrosion Measurements, Princeton Applied Research, Web: www.princetonappliedresearch.com

[8]   Electrochemical Corrosion Test Methods, Quick Reads: Insight on Litigation Technical Investigations for Litigators, IP Attorneys, Insurers, Corporate Counsel,www.FalexInvestigations.com|p: 630.556.9700

INVESTIGATING OF AN HOURGLASS

Fatemeh Janmohammadi, Farzanegan 7 High School,Tehran/Iran , f.jani80@gmail.com

A B S T R A C T

In this research parameters that are effective on an hourglass has been surveyed. Whether or not the weight of a running hourglass differs from the weight of the hourglass at rest is explained by several experiments.

A R T I C L E I N F O

1 Introduction

In order to solve this question, suppose we have a running hourglass which is in its steady state (Fig.1). In this situation on one hand, since a portion of the sand is in free fall, it seems that the hourglass should weigh less. On the other hand, the impact of the sand on the base of the hourglass should increase the downward force exerted on the scale. We want to understand that which effect is greater and how they are acting on each other and investigating some parameters that would have effect on changing the weight of a running hourglass.
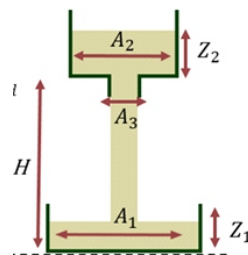

Fig.1: an hourglass in a steady state

2 Theory and Model

We decompose the running hourglass into three states (Fig. 2):
1)the beginning state ,when the hourglass starts to flow until the first bit of sand hits the ground
2)the steady state when both upper and lower chambers contain a portion of sand
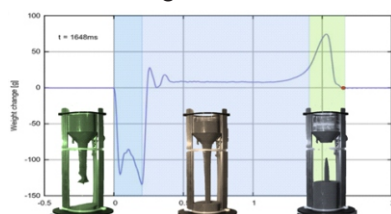3)the end state ,when the last bit of sand leaves the upper chamber until it hits the ground

Fig.2: The running hourglass in three states

In the beginning state we have just free fall and we expect the apparent weight of hourglass decreases. In order to find the total time of this state t_1 and the maximum decreasing weight δW_1 we have to take into account some assumptions. First we assume the flow rate Q reach to a constant M/T where M is the total mass of sand in the hourglass and T is the total time of flowing hourglass[2] .

Second, we assume the sand grains do not have any interaction to each other during the falling. With these two assumptions we can easily find t_1 as the following :

$$H = \frac{1}{2}gt^2 \qquad t_1 = \sqrt{\frac{2H}{g}} \tag{1}$$

where (H) is the distance between the orifice and the ground. Now we can find δW_1 as (eq. 2):

$$\delta W_1 = -\delta M_1 g = -Q t_1\, g = -Q\sqrt{2gh} \tag{2}$$

Therefore we predict a linear decreasing of weight from 0 to $-Q\sqrt{2gH}$ during the time of $\sqrt{\frac{2H}{g}}$ in the beginning state.

In the steady state we have both free fall and impulse at the same time. The total time of this state would be t_2 . In this state we assume the impulse is a pure inelastic impact and the momentum of the sand reaches to zero after hit the ground. Imagine in a typical time t the height of z_1 in the lower chamber is filled. Therefore, the total losing weight would be $-Q\sqrt{2g(H-Z_1)}$ and the force of impact can be obtained by:

$$f_{imp} = \frac{\delta P}{\delta t} = \frac{0-(-\delta mv)}{\delta t} = \frac{Q\delta tv}{\delta t} = Qv \tag{3}$$

on the other hand, from conservation of energy we have:

$$\frac{1}{2}mv^2 = mg(H - z_1) \tag{4}$$

$$v = \sqrt{2g(H - Z_1)} \tag{5}$$

which by substituting the total force of impact would be $Q\sqrt{2g(H-Z_1)}$ so the net deviation of weight in the steady state would be $\delta W_2 = Q\sqrt{2g(H-z_1)} - Q\sqrt{2g(H-z_1)} = 0$ and in the steady state we expect not changing in weight of hourglass.

In the end state, the amount of sand in the free fall will be decrease by passing time but the impulse will still remain. The total time of this state t_3 can be found by the time of free fall of last grain of sand from orifice to the head of lower chamber (z_1) and would be $t_3 = \sqrt{\frac{2(H-z_1)}{g}}$ The maximum increasing of weight due to impulse would be:

$$\delta W_3 = Q\sqrt{2g(H-z_1)} \tag{6}$$

Then, in this state we expect a linear increasing of the weight from 0 to $Q\sqrt{2g(H-z_1)}$ during $\sqrt{\frac{2(H-z_1)}{g}}$ time.

It is a very simple calculation which shows zero changing weight in the steady state but a very important thing that we missed in calculation is the moving of center of mass. We know that the acceleration of the center of mass of a system is equal to the net force on the system divided by the mass of the system. It can be shown that the acceleration of the center of mass of a system in the beginning and end states is ignorable in comparison with other source of weight changing. Therefore we just focus on the acceleration of the center of mass of a system in the steady state. First of all we suppose in a typical time t, when the height of sand in lower and upper chambers are z_1 and z_2. Also, the area of cross sections of lower chamber, upper chamber and orifice are A_1, A_2 and A_3. We assume the sand grains are distributed uniformly in lower and upper chambers, and also in the free fall distributed in a cylinder with area of A_3. With these assumptions the center of mass of system can be find as[1]:

$$z_{cm} = \frac{\rho}{M}\left[A_1 z_1 \left(\frac{z_1}{2}\right) + A_2 z_2 \left(H + \frac{z_2}{2}\right) + A_3 (H-z_1)\left(\frac{H+z_1}{2}\right)\right] \tag{7}$$

$$M = \rho[A_1 z_1 + A_2 z_2 + A_3 (H-z_1) \tag{8}$$

now, we can find the decreasing of mass in upper chamber *mu* by the flow rate as the following:

$$\frac{dm_u}{dt} = -Q \rightarrow \frac{d(\rho A_2 z_2)}{dt} = \rho A_2 \frac{dz_2}{dt} = -Q \quad \frac{dz_2}{dt} = \frac{-Q}{\rho A_2} \tag{9}$$

By getting a differentiation over time from equation (8) and substituting equation (9), we have:

$$\frac{dM}{dt} = \rho\left[A_1 \frac{dz_1}{dt} + A_2 \frac{dz_2}{dt} + A_3 - \frac{dz_1}{dt}\right] = 0 \quad \frac{dz_1}{dt} = \frac{Q}{\rho(A_1 - A_3)} \tag{10}$$

now by two times derivation from :in equation (7) and substituting equations (9) and (10), the acceleration of center of mass can be found as:

$$\frac{d^2 z_{cm}}{dt^2} = \frac{Q^2}{\rho M}\left[\frac{A_1}{(A_1-A_3)^2} + \frac{1}{A_2} - \frac{A_3}{(A_1-A_3)^2}\right] \tag{11}$$

Since we have A1,A2 > A3 then the acceleration is always greater than zero which means it is upward. Then the changing weight in the steady state will be:

$$\delta W_2 = M\frac{d^2 z_{cm}}{dt^2} = \frac{Q^2}{\rho}\left[\frac{A_1}{(A_1-A_3)^2} + \frac{1}{A_2} - \frac{A_3}{(A_1-A_3)^2}\right] \tag{12}$$

3 Experiments

We made the hourglass with two rods, a glass container, a funnel and the gate for controlling the time when we want the grains to pour (Fig. 1).

We filled the upper container with different materials (salt, sand) and we put it on the scale . We took a slow motion film during the experiment .When the sand starts pouring, the weight decreased then It has some fluctuations

and after that It increased (able 1).

Fig. 3: Experimental hourglass

Table 1: Measurements in experimental hourglass

Measurement	
Parameter	Magnitude
A_1	$78.5 cm^2$
A_2	$33.16 cm^2$
A_3	$2.09 cm^2$
h	$52 cm$
ρ(salt)	$1.4\ g/cm^3$
ρ(sand)	$1.8\ g/cm^3$
ρ(iron)	$4.9\ g/cm^3$

The triple beam scale had a short response time but because of its low measurement accuracy we did not see the magnitude of decreasing and increasing of weight that we expected and we did not δW_2 so we made a lightweight hourglass to be able to do our experiment with digital scale that had a good response time and high measurement accuracy, so we saw the magnitude of weight we expected to see δW_2 (Fig. 4 and table 2).

Table 2: Measurements in lightweight hourglass

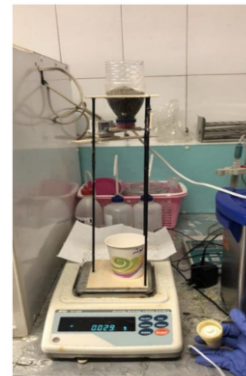| Measurement	
Parameter	Magnitude
A_1	$23.7 cm^2$
A_2	$69.3 cm^2$
A_3	$0.78 cm^2$
h	$34 cm$
ρ(salt)	$1.4\ g/cm^3$
ρ(sand)	$1.8\ g/cm^3$
ρ(iron)	$4.9\ g/cm^3$

Fig. 4: Lightweight hourglass

4 Results and discussion

We can see that height(distance between orifice and the

ground) has an effect on decreasing and increasing of weight. When we have a longer system, the variations of weight would be greater and we can see the same results with different materials . Our materials were sand and salt with different densities which sand is a bit more dense than salt (Fig. 5 a / b; Fig. 6) .
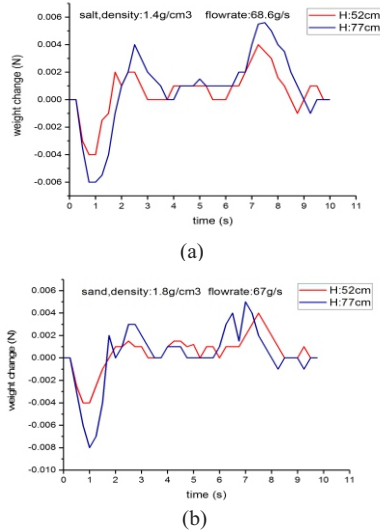

(a)

(b)

Fig. 5: Weight changes versus time in the first hourglass, with different materials a) salt and b) sand
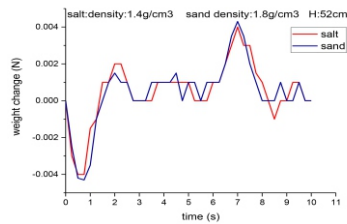

Fig. 6: Weight changes versus time in the first hourglass, comparison of salt and sand

The correct magnitude of changes of weight and δW_2 in two different materials (sand and iron filing) (Fig 7 a/b).
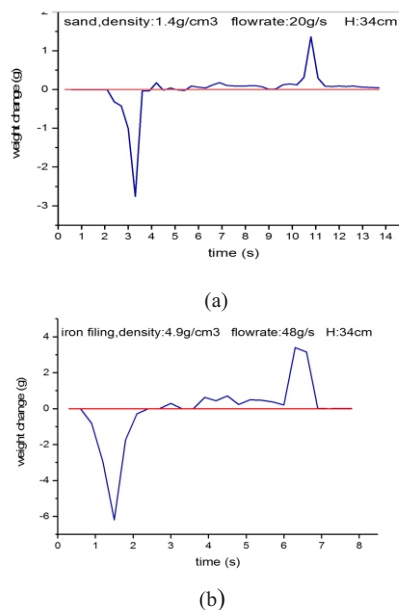

(a)

(b)

Fig. 7: Weight changes versus time in lightweight hourglass with different materials, a) sand , b) iron

5 Conclusion

When we have a material with greater density, fluctuations of weight at first and at the end (even in the steady state that we can not see because of low measurement accuracy of scale) will be greater. In the first setup ,the changes of weight are not exactly match with the numbers in our theory and we did not see δW_2 because of the low measurement accuracy of triple beam scale.

The results from the second setup (the lightweight setup and digital scale) show the correct magnitude of changes of weight and δW_2 in two different materials (sand and iron).

We have some other effective parameters in this phenomenon which can affect on changing the weight of it .By increasing the area of A_1 and A_2, the changing weight will decrease. On the other hand by increasing the area of A_3 the flow rate (Q) will be increased and then the changing weight will be increased too. By increasing the density ρ the flow rate Q will be increased and then the changing weight will be increased too.

References

[1]   Haliday D., Resnik R. ,Walker J.,1923. Fundamental of physics.John Wiley and sons.

[2]   Sack A., and Pöschel T., 2017. "Weight of an hourglass Theory and experiment in quantitative comparison." American Journal of Physics 85.2 : 98-107

GEE HAW WHAMMY DIDDLE

Rozhina Sedigh, Farzanegan 2 High School, sedighrozhina@gmail.com

A B S T R A C T

Dynamics are investigated for a rigid spinner with a hole, concentric with its mass center, into which a pivot is loosely fitted. Gee haw whimmy diddle is a mechanical toy, which by rubbing a stick rapidly back and forth on the notches, it causes the propeller to rotate.

A R T I C L E   I N F O

1 Introduction

"Gee-Haw" refers to the fact that, by rubbing your finger against the notched stick while rubbing, the direction of the spinning propeller may be reversed. The operator may do this surreptitiously and yell "Gee" or "Haw" to make it appear that the propeller is reacting to the commands. If you call it a "Hooey Stick", you would yell "hooey" each time you want the direction to change. Different relevant parameters on the angular velocity of the propeller; such as difference, in the size of the stick, shape of the notches, size of the propeller, material of the stick, size of the hole, geometry of the stick and the number of the notches were investigated and...

back and forth vibrations in the notched pencil as you run the second pencil over it. These horizontal vibrations have a specific oscillation pattern that creates vertical or up and down vibrations in the pin. The pin's vertical vibrations take the form of circular or elliptical motion, and this motion causes the propeller to spin was observed...
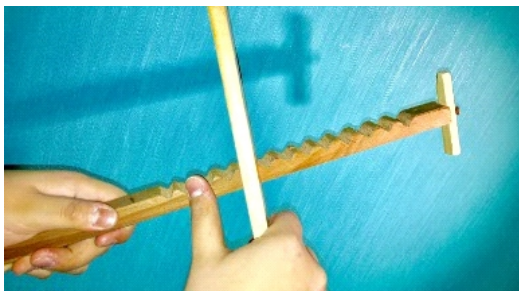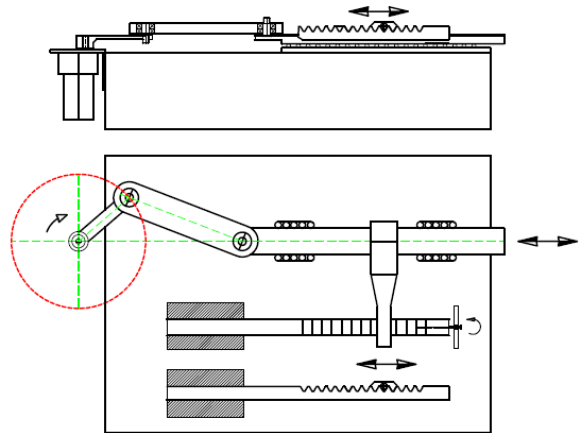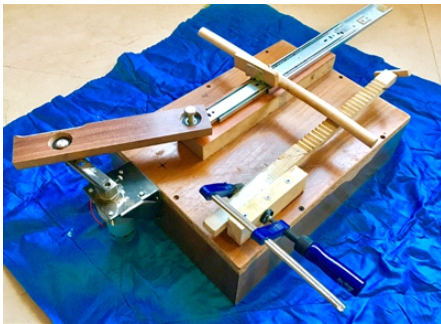
2 Theory

The spin of the propeller is caused by horizontal or

MAGNETIC TRAIN

Zahra Moghimi, Farzanegan 3 High School,Tehran/Iran

A B S T R A C T

Magnetic train as one of the IYPT 2016 problems contains a battery with two attached permanent magnets in both ends of it; when put in solenoid it moves. Why this train moves and relevant parameters have been studied to find its best efficiency and the effect of some relevant parameters on speed and power with considering electromagnetic laws. Using simulation and formulas help to study more on magnetic fields in the whole train.

1 Introduction

The theory discussed in this paper is around the battery with two permanent magnets that attached to the both ends of the battery. When you put them in a copper coil will be moved through the solenoid.

Will Robertson *et al*., worked about calculating axial force between a coaxial cylindrical magnet and a thick coil (a solenoid that its thickness should considered and isn't negligible) with relative displacement in axial direction. This theory is in both theoretical and analytical type with two different way of calculating and formulas [1].

2 Theory

For two circular coaxial loops (i.e., a single turn of a solenoid) carrying currents, the axial force between them is given by:

$$F_f(r_1, r_2, z) = \mu_0 I_1 I_2 z \sqrt{\frac{m}{4 r_1 r_2}}$$
$$\times \left[K(m) - \frac{m/2 - 1}{m - 1} E(m) \right] \qquad (1)$$

$$m = \frac{4 r_1 r_2}{[r_1 + r_2]^2 + z^2} \qquad (2)$$

Where r_1 and r_2 are the coil radii z and is the axial distance between them. The functions $K(m)$ and $E(m)$ are the complete first and second elliptic integrals respectively with parameters. These functions can also be referred to with notation $K(k)$ and $E(k)$ in terms of a modulus k_1 where $m = k^2$. Using the "filament method," (1) and (2) can be used to calculate the force between any arrangement of coaxial solenoids by representing each turn of the solenoid as a separate coil, and summing the forces through superposition for every pair-wise combination of coil interaction forces.

$$F_{z_1} = \sum_{n_m=1}^{N_m} \sum_{n_r=1}^{N_r} \sum_{n_z=1}^{N_z} F_f(r(n_r), R_m, z + L(n_m, n_z)) \qquad (3)$$

$$r(n_r) = R_c + \frac{n_r - 1}{N_r - 1}[R_c - r_c] \qquad (4)$$

$$L(n_m, n_z) = -\frac{1}{2}[l_m + l_c] + \frac{n_z - 1}{N_z - 1} l_c + \frac{n_m - 1}{N_m - 1} l_m \qquad (5)$$

where R_m is the magnet radius , r_c and R_c are the inner and outer coil radii, lm and lc are the magnet and coil lengths, z is the axial distance between their centers, N_r and N_z are the number of turns in the thick coil in the radial and axial direction, and N_m is the number of turns in the thin coil.

Flexible algorithm is calculated for accurate computation of off-axis magnetic fields of coil in cylindrical geometry (Robert H. Jackson *et al.*).

This calculation was about a partial power series decomposition of Laplace's equation about the symmetry axis where the series coefficients are derivatives of field along the axis and computed for basic coil type (loop, annular disc, thin solenoid, full coil) with high order analytic derivatives [2] and the general vector field inside a real (finite) solenoid has been studied by: (R. Muniz *et al.*, 2015) (Fig. 1)[3].
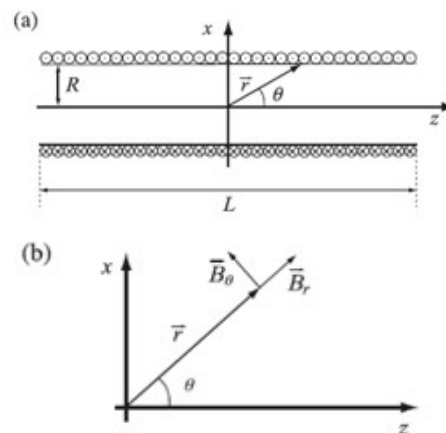

Fig. 1: The vector field inside a real (finite) solenoid

$$B_\rho \simeq \frac{3\alpha L R^2 r^2}{2(R^2 + L^2/4)^{5/2}} \sin\theta \cos\theta. \qquad (6)$$

Finally, using q ¼ r sin h and z ¼ r cos h :

$$B_\rho(\rho, z) \simeq \frac{96\pi NI}{c} \left(\frac{R^2 z \rho}{L^4} \right),$$ (7)

Here, we introduced a magnetic train moves in a solenoid and surveyed the relevant parameters and measured its velocity and power too.

3 Material and Methodology

Because of the current in wire there is a magnetic field around it. In our setup the permanent magnet and the battery produce current in solenoid. When a current passes from the solenoid a magnetic field is produced in and around of it and with right hand rule, the north and south poles will be set. If the opposite poles of permanent magnets are outwards, the poles will attract the opposite pole of the solenoid so the vectors of magnetic force will be in opposite direction and its resultant vector will be zero (Fig.2).
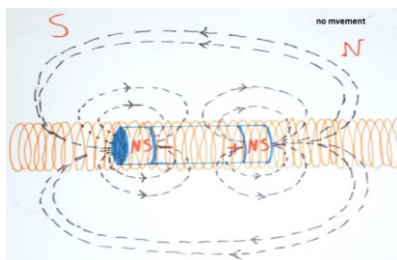

Fig. 2. :The fields of train when there is no movement

But if the same poles of permanent magnets are outwards; one of the poles will attract the opposite pole of the solenoid's field and another pole repulse the same pole of it so the vectors of magnetic force will be in the same direction and it's resultant vector will not be zero. It means that just if same poles of magnetic train are outwards the interaction of these three fields is in a way that train moves (Fig. 3).
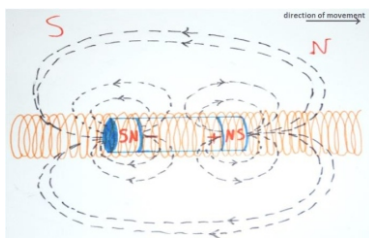

Fig. 3 : The fields of train in a correct way that moves

and it is important to realize that the solenoid is a thick coil with the fields in it. Until going the battery out of solenoid, there is a field around it and make a continuous movement for train (Fig.4).
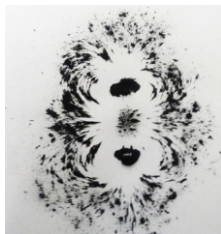

Fig. 4: Field of battery with its attached magnet

There is a force that reduces the speed of train or sometimes makes it stop. There is some spaces between wires of solenoid when the train moves through the solenoid and passes these spaces, the edge of train sticks in this spaces. A force perpendicular on the wire and the edge of train avoids train from movement (Fig. 5).
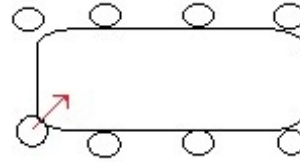

Fig. 5.: The direction of the force that reduces the speed of train on the edge of train

4 Experiments

The set up in our experiments has been built with four thin threads that make the length of solenoid constant, two short cardboards in both sides of solenoid to avoid shaking and a paperboard under it to avoid make any contact with other conductive surface, 9 disc magnets and two types of battery: NiMH rechargeable battery and alkaline (Fig. 6).
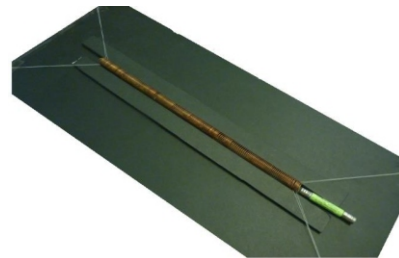

Fig. 6: experimental set up

According to electromagnetism laws the force between two magnets are measured .

There is an inducted field in solenoid as a permanent cylindrical magnet. The force between two magnets are equal to force between an iron and a magnet [4] so the force between magnet that attached to battery with battery is equal to the force between two magnets. To make the train move we must attach four or five disc magnet to each other because they aren't powerful enough lonely so they behaves like a cylindrical magnet that force between them and the solenoid is measured (Eq. 8) [4,5,6]:

$$F(x) = \frac{\pi \mu_0}{4} M^2 R^4 \left[\frac{1}{x^2} + \frac{1}{(x+2h)^2} - \frac{2}{(x+h)^2} \right]$$ (8)

Where M is the magnetization of the magnets and x is the distance between them. However, we have an attraction and repulsion, too; that is measured with (Eq. 9).

$$F = \frac{\mu q_{m1} q_{m2}}{4\pi r^2}$$ (9)

Where F is force, q_{m1} and q_{m2} are the magnitudes of magnetic poles , μ is the permeability of the intervening medium , r is the separation .

5 Simulation

As it mentioned before; our solenoid is a thick coil because the current just passes around the train, so the magnetic field just inducted around the train, not in the whole solenoid. The field in solenoid is less homogenous

density in the thick coil is more than around of it; so the speed of train inside the solenoid is more . We put the train in the solenoid and simulated the thick coil's magnetic field using COMSOL Multiphysics. The simulation is in elementary steps and the whole train will simulated in future (Figures 7 and 8).
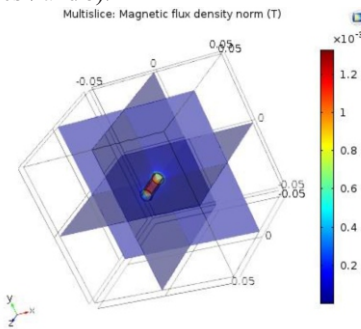

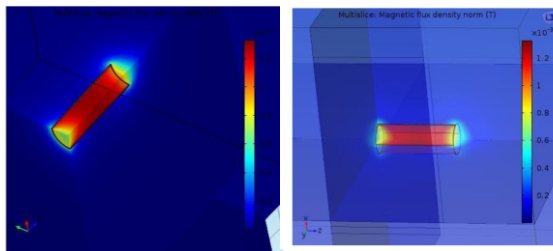**Fig. 7:** outlook of simulation

Fig.8: closeup of the magnetic field of the thick coil

The compression of wires in the solenoid is 5.413±0.05 mm in each centimeter. Material of solenoid is copper because it has high electric conductivity. The thickness of wire is 1.16±0.005 mm and internal diameter of solenoid is 13.42±0.005 mm (tables 1 and 2).

Table 1 : Batteries are used in our experiments

battery	Thickness (mm)	Length (mm)	Internal resistance (Ω)
(alkaline)	10±0.05	42±0.05	1.02±0.005
(NiMH)	10±0.05	43±0.05	0.84±0.005

Table 2 : Magnetic fields, measurements with magnetometers software

magnet	Magnetic field(μT)	Thickness (mm)	Radius(mm)	number
	855±0.1	4±0.05	5±0.05	1
	560±0.1	2±0.05	5±0.05	1
	1012±0.1	5±0.05	5±0.05	2
	653±0.1	3±0.05	5±0.05	5

6 Results

The experiments and all results are shown in the following figures. By increasing current; speed increases, too (Fig. 9).
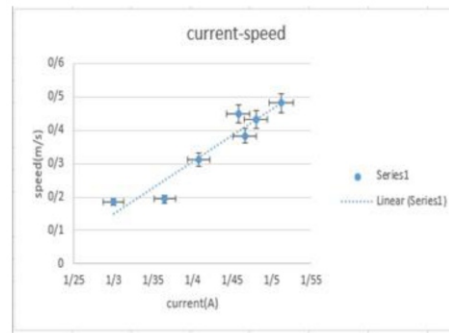
Fig. 9: the speed versus current with alkaline battery

By increasing current, power increases, too (Fig. 10).

Fig. 10: power versus current with alkaline battery

Fig. 11: power versus voltage with alkaline battery

Fig.12: Speed versus current with NiMH battery

Fig.13: Speed versus voltage with NiMH battery

According to these charts and formulas, the relations between these parameters are linear. By increasing voltage and current, power and speed will increase, too.

For better efficiency, we can use batteries with higher voltage and current, less mass and make the solenoid smooth to avoid forces that decrease the speed.

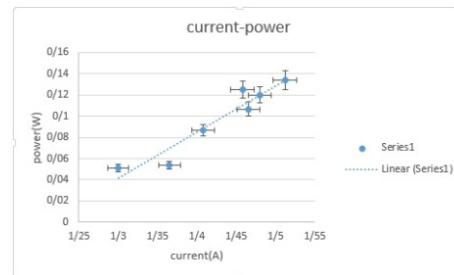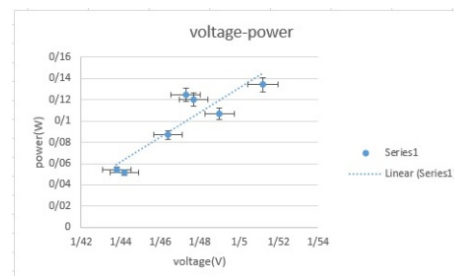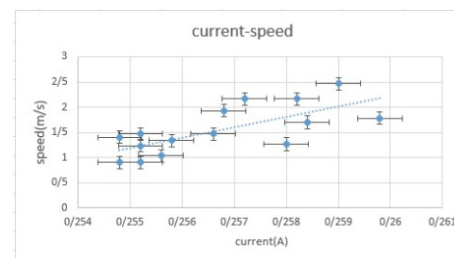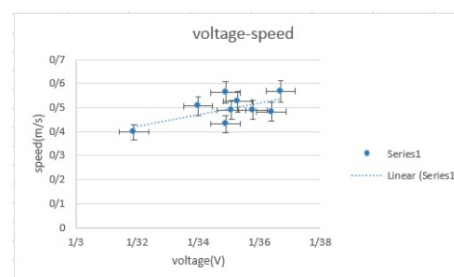## 7 Conclusion

Magnetic train moves with magnets attached to the battery from the same poles and in a copper coil. It is better to put train in the solenoid because the magnetic flux density is more in the solenoid than around of it . Our solenoid is a thick coil because the field is inducted just around the battery and moves with it through the solenoid that helps train to move along the whole solenoid. Every parameter that makes the fields powerful can improve efficiency. As shown in figures, with increasing voltage and current; power and speed increases too and there is a linear relation between them. For increasing efficiency, the easiest way is increasing current because it has most effect to make the field of coil powerful.

References

[1]   Robertson W., Cazzolato B. and Zander A., Axial Force Between a Thick Coil and a Cylindrical Permanent Magnet: Optimizing the Geometry of an Electromagnetic Actuator. School of Mechanical Engineering, The University of Adelaide, SA 5005, Australia. personal.mecheng.adelaide.edu.au/will.robertson/research/2012-magcoil.pdf

[2]   Jackson R. H. , 1999.   Off-Axis Expansion Solution of Laplace's Equation: Application to Accurate and Rapid Calculation of Coil Magnetic Fields. IEEE TRANSACTIONS ON ELECTRON DEVICES , VOL. 46, NO. 5,

[3]   Muniz S. R. , Bagnato V. S., and Bhattacharya M. , Analysis of off-axis solenoid fields using the magnetic scalar potential: An application to a Zeeman-slower for cold atoms, https://arxiv.org/abs/1003.3720

[4]   David J., 1998. Introduction to Electrodynamics(3rd ed.). Prentice Hall. ISBN 0- 13-805326-X., section 6.1.

[5]   "Basic Relationships". Geophysics.ou.edu. Retrieved 2009-10-19, https://www.revolvy.com/page/Magnet

[6]   "Magnetic Fields and Forces". Retrieved 2009-12-24, https://wikivisually.com/wiki/Force_between_magnets

WATER BOTTLE FLIPPING

Sorin Yousefnia , Farzanegan 7 High School,Tehran/Iran, sorinyousefnia81@gmail.com

A B S T R A C T

The current craze of water bottle flipping involves launching a partially filled plastic bottle into the air so that it performs a somersault before landing on a horizontal surface in a stable, upright position. Investigate the phenomenon and determine the parameters that will result in a successful flip. The secret behind a success flip of a water bottle into the air, is the distribution of mass, decreasing the angular velocity and finally landing like a shuttle cock,   in this way for solving the problem easier we divided the hole system to 3 phases: Damping, Landing and Impact.

A R T I C L E   I N F O

1 Introduction

In water bottle flipping as a challenge, the most important parameters which can result in the best and successful landing, are investigated.

First of all let's talk about the amount of water and how important it is. When the amount of water in a bottle is very little or almost full, most of the energy in hitting the ground will be transferred to the bottle then there is a bounce back without a success flip. But in a bottle with enough water, some of the energy will be transferred to the water and without a bounce back there is a successful flip.

When we throw a water bottle into the air, a success flip is because of the distribution of mass and decreasing the angular velocity . To solve the problem the hole system is divided to three phases: Damping, Landing and Impact (Fig. 1).
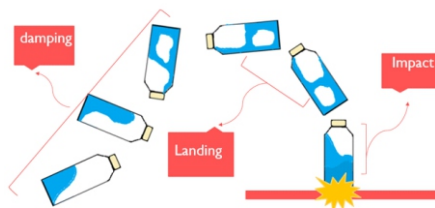

Fig. 1: 3 phases in throwing a water bottle

2 Theory

To find the moment of inertia around the center pf mass of the hole system (CM), the hole system is divided to 2 parts, water and bottle .
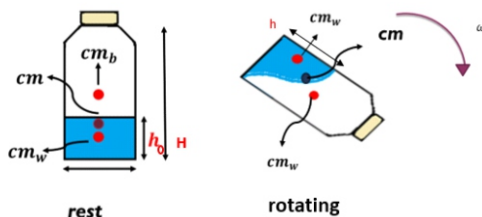

Fig. 2: Center of mass in two different situations, rotating and resting

In this case when bottle is completely empty or full the center of mass will be equal with H/2 .

$$h_{cm} = \frac{\frac{H}{2}m_b + \frac{h}{2}m_w}{m_b + m_w} = \frac{H}{2}\left(\frac{m_b + m_w \frac{h}{H}}{m_b + m_w}\right) \tag{1}$$

$$I_b = \frac{1}{12}m_b H^2 + m_b \left(\frac{H}{2} - h_{cm}\right)^2 \tag{2}$$

$$I_w = \frac{1}{12}m_w h^2 + M \left(\frac{h}{2} - h_{cm}\right)^2 \tag{3}$$

$$I = I_b + I_w \tag{4}$$

According to the conservation of angular velocity, the minimum angular velocity is the angular velocity of the water plus the angular velocity of the bottle .

$$I_0 \times \omega_0 \approx I_{max} \times \omega_{min} \tag{5}$$

$$\omega_{min} \approx \frac{I_0}{I_{max}} \times \omega_0 \tag{6}$$

3 Modeling and Experiments

To decrease the errors and the same initial conditions, a mechanical setup was built to hit the bottle (Fig. 3).

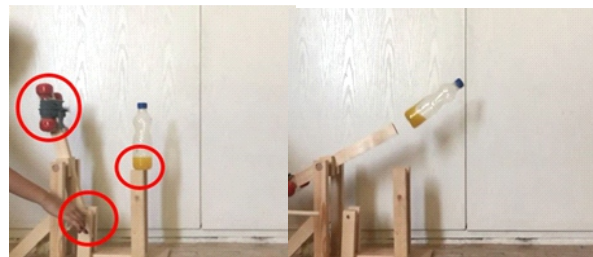**Fig.3:** Mechanical device for throwing the bottle

The bottle with changing the amount of water acts as different objects, sometimes like a rigid object which moment of inertia is constant without having distribution of mass but in other occasions there is distribution of mass [1].

While bottle is flipping, the water needs a place to apply a force and support it from the centripetal force. In low

amount of water, the bottom of the bottle is able to apply the force so water won't move a lot. In high amount again the walls and bottom of the bottle are able to apply the force and support it, so in this situation water won't move almost. But when it is partially full of water a free space is seen during flipping (Fig. 4)

Fig. 4: Flipping with different amount of water

To decrease ω ,we can first decrease ω_0 but it is impossible because if we decrease it a lot we won't even have a flip so the best and maybe the only way is decreasing the amount of $\frac{I_0}{I_{max}}$ and as in figure (5) the minimum part causes flipping [1,2].
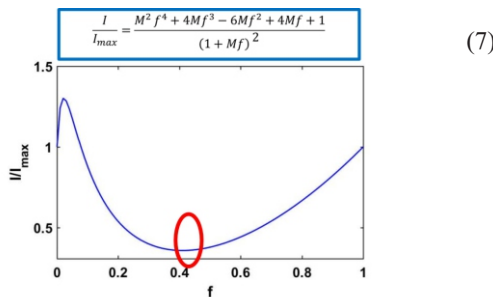
$$\frac{I}{I_{max}} = \frac{M^2 f^4 + 4Mf^3 - 6Mf^2 + 4Mf + 1}{(1+Mf)^2} \qquad (7)$$

Fig. 5: The minimum part that rotational velocity is minimum

4 Results

Comparing to the theory, the rotational velocity of successful flip should decrease about 60% but in these experiments it decreased about 80% because the energy has been transferred to the water .
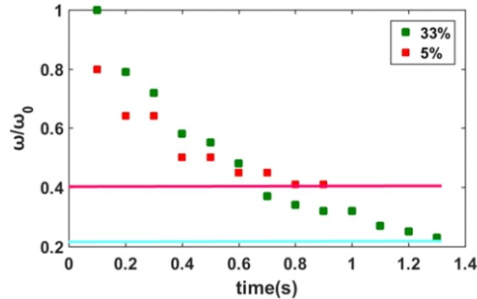

Fig. 6: The red line shows the amount that it should decrease according to the theory and the blue one shows the deduction according to the exp. And this difference shows transferred energy to the water

The second phase (Landing) is the same as shuttlecock. When we throw a shuttlecock without a rotational velocity, it comes down with its heaviest part and hit the ground in a stable upright position.
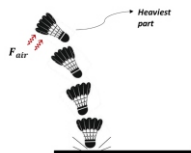

Fig. 7: Landing a shuttlecock considering air resistance

The amount of water and the center of mass will help the bottle to find a stable upright position in landing as the last phase (Fig. 8).

$$\frac{h_{cm}}{H} = \frac{1}{2}\left(\frac{1+Mf^2}{1+Mf}\right) \qquad (8)$$
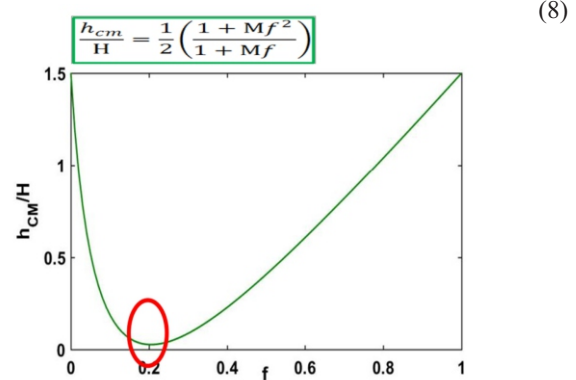
Fig. 8: The minimum shows the best position for landing

Bottle with M=14 shows two minimum parts, which is assumed the best situation and the most successful parts should be there because the rotational velocity is minimum and also the CM is very low too (Fig. 9)[2] .
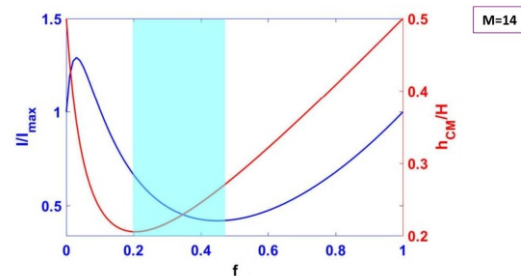
Fig. 9: Bottle with M=14 and two minimum parts

Let's compare the theory with our experiments . The best given results are exactly in that place but we have a little error because of our assumptions (Fig. 10)[2, 3].
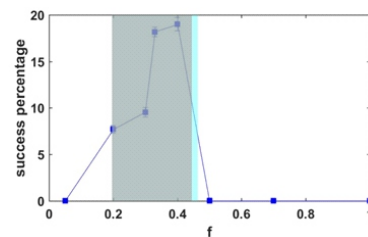
Fig. 10: The best situations comparing by theory and experiments

The other effective parameter is surface. Three different surfaces show the softer gives the better results because when it is hard, stone for example, we will have bounce back and a big amount of energy will be transferred to the bottle (Fig. 11).
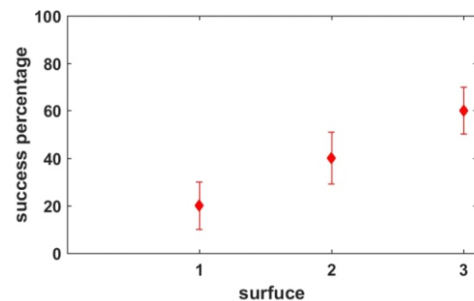
Fig.11: Success percentage in 3 different surfaces

   Now by changing the amount of D/h, the diameter of the bottom to the height of the bottle, the results were examined. By increasing this amount, more successful was found because in the most situations CM isn't in front of the edge (Fig. 12).
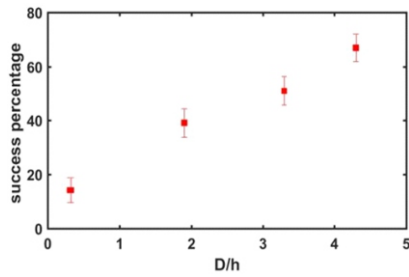
Fig. 12: Success percentage versus D/h

5 Conclusion

By investigating the phenomenon and comparing theory and experiments we found the best situations for having a successful flip:

    1.we should decrease the rotational velocity

    2.We should decrease the amount of center of mass

    3.having an enough free space and movements of water by the centripetal force

    4.having distribution of mass

    5.increasing the D/h

    6.making the surface soft

    7.having optimal filling friction between $0.2 - 0.45$

    8.Landing like a shuttlecock

References

[1]   Halliday D., Fundamentals of physics

[2]   Fowles G. R. and Cassiday G. R. , Analytical Mechanics

[3]   Dekker P.J. and L.A.G Eek et al, Flapper M.M., Horstink H.J.C., Meulenkamp A.R., Meulen J., Kooij E.S., Snoeijer J.H., Marin A. (2017). Water Bottle Flipping Physics, The Netherlands 2 Physics of Interfaces and Nanomaterials.

THE RING OILER

Hirad Davari , Rahe Roshd High School,Tehran/Iran, hirad.davari@yahoo.com

ABSTRACT

When a ring is put on a horizontal cylindrical shaft, it start to rotate around its axis at constant speed. It can travel along the shaft in either direction depending on the tilt of the ring. In this article we are going to investigate this phenomenon which was presented in IYPT 2018. We are going to investigate the phenomenon in a case were the ring is made of cardboard and the shaft is oiled. The reason behind the motion at the first place regarding to the microscopic point of view is explained that the motion of the shaft is intrinsic of the shaft and the rings circular shape. A mathematical model is used to clarify this phenomenon accurately.

1 Introduction

An oiled horizontal cylindrical shaft rotates around its axis at constant speed. Make a ring from a cardboard disc with the inner diameter roughly twice the diameter of the shaft and put the ring on the shaft. Depending on the tilt of the ring, it can travel along the shaft in either direction. This is IYPT 2018 problem which is investigated .

The first step is to explain why the ring moves along the shaft's axis in the first place. This is possible by taking a close microscopic look. Think of the ring at a set of particles, regarding the fact that both the ring and the cross section of the shaft are circular they only intersect in one point. However due to the imperfect shape of the shaft's surface and the ring's inner surface, this point extends to a small area (Fig. 1) which we call the contact area.
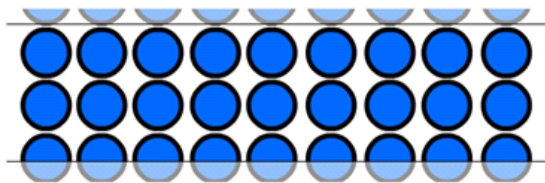

Fig . 1: the shaft can be thought of as a group of particles (shown in picture as circles). The ring and the shaft intersect in a small area called the contact point (the opaque area in between the two lines).

2 Theory and Methods

By looking at the particles of the ring as a set of particles too and a bit of simplifying we conclude that the particles of the ring tend to move in the direction towards which the particles of the shaft are moving as if they are "attached" to those particles by static friction. This kind of motion causes the particles of the ring, to repeatedly enter and exit the contact area. The new particle which enters the contact area is a bit to the side which is because of the tilt of the ring (Fig. 2) which perfectly explains why the ring moves to the side.

In figure (2a) the particles of the ring and the particles of the shaft move in the same direction and the same velocity due to the static friction between them. The two particles, A

and B, are indicated. A, lays inside and B lays outside of the contact area. As shown in figure (2b) particle A is dragged outside and particle B is dragged into the contact area. Notice that particle B is a bit to the left due to the tilt of the ring. As explained in figure (2c) the transformation is endless due to the circular shapes of the ring and the cross section of the shaft and the points in contact (highlighted) keep changing. This causes the ring to move to the side.

(a)   (b)

(c)
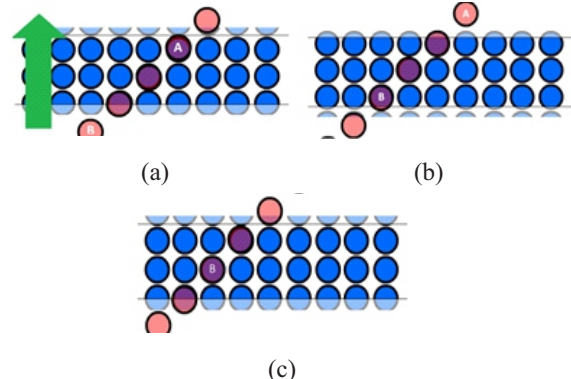
Fig. 2.a) The light colored circles represent the particles of the ring; b) particles A and B, They have both been displaced in the direction the shaft is rotating; c)The transformation is endless

Now let's have a look from the top. According to $\vec{v}$ ıat was said, the particles of the ring move with a velocity $\vec{v}$ in the direction the shaft is rotating. We can rewrite this vector as two other velocities. Let v_r be the velocity vector which is in the direction of the ring and v_x be the velocity vector in the direction of the shaft(Fig. 3).

Fig. 3: The vectors of the velocity in rotating shaft

We know that the ring can't move in the direction of v_r hence this velocity only makes the ring revolve about its

own axis and v_x is the velocity of its linear motion. From the above explanation we have [1]:

$$v = v_r.\cos\alpha => \omega_s.r = \omega_r R.\cos\alpha => \omega_s = \omega_r.\times\frac{R}{r}\cos\alpha \quad (1)$$

where ω_r and ω_s are the rotational velocities of the ring and the shaft and r and R are the radius of the shaft and the ring respectively.
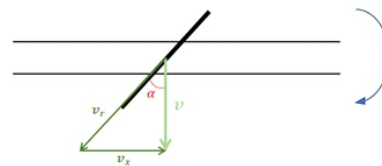
As the problem lets us assume that $\frac{R}{r} = 2$ we could write:

$$\omega_r = \frac{\omega_s}{2\cos\alpha} \quad (2)$$

$$v_x = v.\tan\alpha => v_x = \omega_s r.\tan\alpha \quad (3)$$

Here we can define the degrees of freedom of the rings motion which are:

v_x : Velocity of the rings linear motion

α : Angle between the rings orientation and the perpendicular line to the shafts length

ω_r : Rotational velocity of the rings revolving motion about its own axis.

Here, we assumed that the particles of the ring and particles of the shaft are attached and move with the same velocity called the critical velocity. However, we know that when the ring is released it doesn't have an initial velocity and slips along the shaft so it accelerates in the direction of the kinetic friction between them [2]. This force causes the ring to move in the direction of the force for a little time before the contact point moves slightly to the back of the ring causing the normal force to cancel out motion (Fig. 4 a/c).
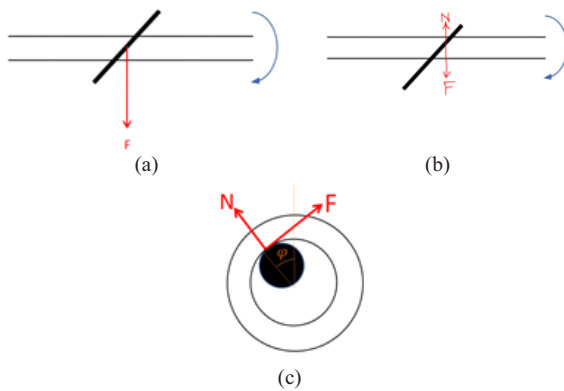

(a)   (b)

(c)

Fig. 4: a:) At the point when the ring is released on the shaft; b) After the ring in the direction of (F) the contact point moves a bit to the back of the ring giving a bit of angle to the normal force so that it cancels out the motion in the direction of F; c)from the side view

When the ring is released as shown in figure (4a) the kinetic friction force (F) gets applied to it, and the normal force is perpendicular to the viewing plane . From the figure (4c) it is clear how the ring has moved to the right and that the angle φ has appeared [3].

On from this point we use the force balance to approach the accelerating motion [3]. After that, we can break the friction force into two components, one of them –in the direction of the ring- causes the torque which makes the ring revolve around its own axis and the other, accelerates the ring. As the contact point has moved a bit to the back, the component of the normal force cancels out the perpendicular component of the remaining force component which later leaves us with a component of force, in the direction of the shaft which accelerates the ring until it reaches the limit velocity -v_x- (Fig. 5a/d).
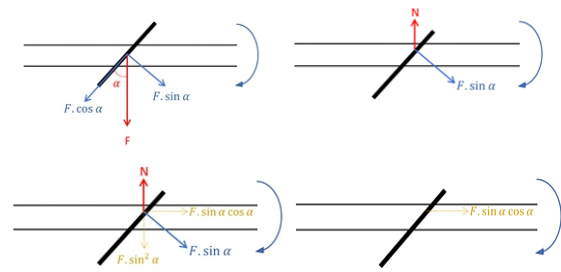
Fig. 5: a) breaking friction into two components one of which causes the torque which makes the ring revolve and the other causes the rings linear acceleration; b) due to the rings dislocation, the normal force has changed direction; c) dividing the remaining friction component into two new components, the perpendicular component must be canceled out by a component of the normal force as the ring is stabilized along that axis; d) one component of friction which accelerates the ring in the direction of the shaft.

Notice the direction of the friction force. The reason why a force in that direction could cause acceleration in the perpendicular direction is the interactions between the ring's linear and rotational movements the same way as the velocities did [2].

- $F.\sin\alpha\cos\alpha = ma$ (4)
- $Fr.\cos\alpha = I\dot{\omega}$ (5)
- $Fr.\sin\alpha\cos\alpha\sin\varphi = I\ddot{\alpha}$ (6)
- $F.\cos\alpha = mg.\sin\varphi$ (7)

By the equations we can calculate the third degree of freedom α .

The phenomenon could be divided into two main states:

1. Acceleration state: from the time when the ring is released until when it reaches the steady state. This is when the ring is accelerating.

2. Steady state: when the ring particles reach the velocity of the shaft and get attached to them.

During our experiments we sometimes observed that the ring changed directions randomly and started moving in the opposite direction without colliding to the side walls of the apparatus . We were surprised by this and succeeded to explain it by the changes of α .

Solving the differential equation (6) we can get the alpha per time plot and due to the fact that during the steady state, friction force disappears and regarding to Newton's first law of motion, the changes of alpha per time are linear in this state(we can draw the implicit plot of α per time like figure 6).
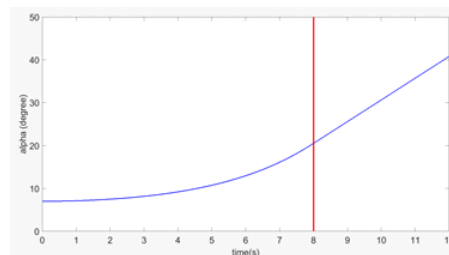
Fig. 6: the implicit alpha per time plot. Starting from the initial angle of 8 degrees and switching to the steady state after 8 seconds (the changes of alpha after that are linear)

This means that the angle between the ring and the shaft keeps decreasing over time. However this transformation cannot happen for ever. When the angle between the ring and the shaft gets lower than a specific value, the inner area of the ring hits the sides of the shaft and applies an impact. Reaction of this impact turns the ring in the opposite

direction that causes this phenomenon which we call sudden rotation(Fig. 7).

(a)   (b)

(c)

Fig. 7 : a) the ring has accelerated and entered the steady state. The angle between the ring and the shaft is decreasing constantly. b) the angle can only decrease down to a point and a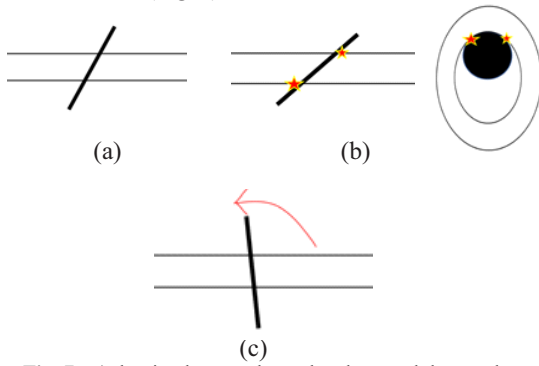fter that it hits the sides of the shaft. By taking a look through the shaft, we can understand this phenomenon easier (right side picture). At this point, a normal force gets applied to the ring at the indicated point which causes an impact. c) After the impact the force applied to the ring makes the ring to turn in the other direction, again with constant rotational velocity. Notice that the direction of the linear motion changes accordingly.

We continue by investigating the effect of different parameters. The effective and investigated parameters were [4]:
1. Side thickness of the ring
2. Air resistance
3. Oil
4. Material of the shaft

Which we are going to investigate here one by one.

2-1 Effect of the side thickness of the ring

We know that the surface of the ring and the shaft are imperfect and that our experiments have error. These errors are cause by many reasons. One of them is the bumpy and uneven surface of the ring. Mention the fact that the ring is cut from cardboard, cutting a perfect circle is close to impossible. Having this said one effect the side thickness has on the general function of the machine is increasing the random effects and errors in the run. The other effect is increasing the chance of sudden rotation because obviously, the minimum angle between a thin ring and the shaft is way less than the minimum angle between a thick ring and the shaft(Fig. 8).
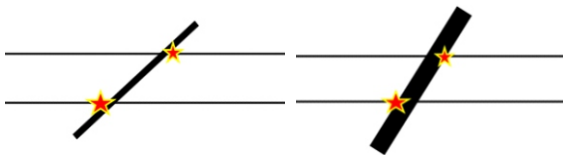

Fig. 8: Comparison between the minimum angle for a thick ring and a thin ring

2-2 Effect of air resistance

Due to the fact that the rings linear motion doesn't have a remarkably high velocity, the air colliding with the ring can smoothly steer along it. This causes the greatest amount of force to be applied to the top corner of the ring (Fig. 9). This force creates a torque and an acceleration backwards. Our experiments show that the effect of the torques is fairly negligible, whereas the acceleration, can lead to another phenomenon.

Suppose the ring is in steady state, the particles of the ring and the particles of the shaft are moving with the same

velocity, however this external, air resistance force causes the particles of the ring to accelerate backwards and stay behind from the particles of the shaft. This puts the ring back into the accelerating state, causing the kinetic friction and most importantly, the angle φ keeps changing which proves our assumptions on the effect of air resistance.
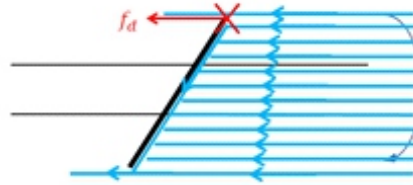

Fig. 9: the greatest amount of force to be applied to the top corner of the ring

2-3 Effect of Oil

We already know as a fact that the surfaces of the ring and the shaft are imperfect. The added lube can fit into the tiny microscopic gaps and decrease the error to a significant extent. This makes both the surfaces smoother thus deceases the kinetic friction coefficient and, as a result, the kinetic friction[1] .This makes the time that the ring spends in the accelerating state longer and omits the errors caused by great force. For example, it was observed that the ring would move forward too much and the angle φ becomes close to a right angle due to the high impact caused by the interior shape. The normal force in this case, applies an impact which makes the ring to bounce and detach from the ring for a moment which is considered as an error. The other effect of adding a lube is taking advantage of the surface tension. Stickiness of the oil causes the particles of the ring and the shaft to stick better to each other. In other words, we could say it increases the maximum static friction. This can limit the effects of environmental forces such as air friction or minor shakes of the setup. To prove this we have done some experiments without using oil, it is observed that the ring frequently bounced up and down on the shaft and we couldn't apply our theory because the ring and the shaft weren't attached anymore.

2-4 Effect of changing the material of the shaft

The main effect of changing the material means the changes of friction coefficient. These changes show themselves in changes of the angle φ .This comes from mathematical ratiocination below:

$$mg = N.\cos\varphi + F.\sin\varphi \tag{8}$$

$$F.\cos\alpha = mg.\sin\varphi \tag{9}$$

$$F = \mu.N$$

$$\mu = \frac{\tan\varphi}{\cos\alpha} \tag{10}$$

3 Experiments

Following the given instructions we constructed the apparatus. It consisted of an iron shaft resting between, two holes cut through a wooden body. The shaft was attached to a high speed electric motor which was connected to a speed controller and by that to a power source. This meant that we were able to alter the rotational velocity of the shaft by controlling the speed controller. As the question has asked us to, we cut rings out of a cardboard disc with a variety radiuses and side thicknesses. To reduce the error caused

by the bumpy inner-surface of the ring we used a hot, circular piece of metal to burn out the extra parts and make the inner surface of the ring as ideal as possible. The setup was then placed on a reasonably leveled surface, measured by an electronic level. Two cameras recorded each run from the top view and the view through the shaft at the same time. We took the slow motion videos of the two cameras and used tracker to track the motion of the ring. The attributes we tracked were:

1- v_x , the linear velocity of the ring
2- ω_r, the rotational velocity of the ring
3- α ,the complement of the angle between the ring and the shaft

And the variables of experimentation were:
1. The outer diameter of the ring
2. The side thickness of the ring
3. Presence or absence of oil
4. Length of the shaft

4 Results

4-1 Graphs and types of data

Five types of data are processed. The position , velocity, alpha and omega per time are shown in figures (10- 13) according to the parameters in table (1).
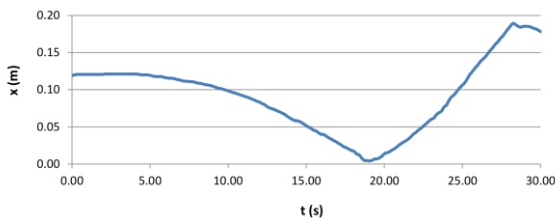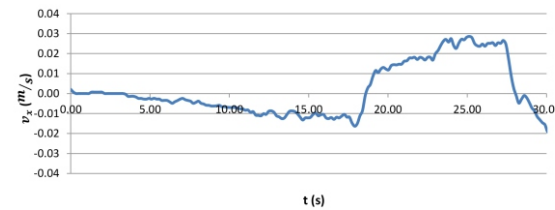
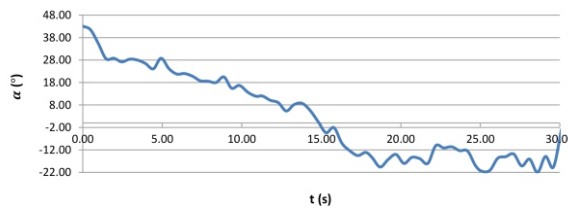**Fig. 10:** Position versus time

Fig. 11: Velocity versus time

Fig. 12: Alpha versus time
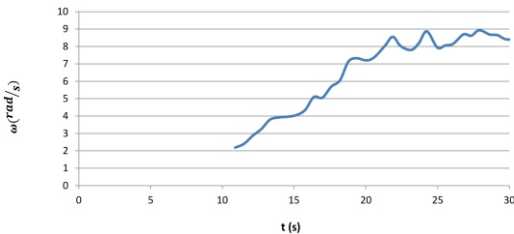
Fig. 13: Omega versus time

Table 1: Measured parameters in experimental setup

Shaft length	19cm
Mass of the ring	5 grams
Outer diameter of the ring	5 cm
Diameter of the shaft	0.9 cm

Figure (2) is taking the derivative of figure (1) but the rest of the graphs are direct data from tracker.

4-2 Theory precision:

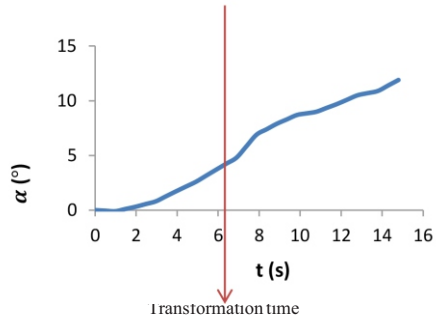The real values and results from theory are compared in figures (14 - 16).

Transformation time

Fig. 14: The values of the alpha by Eq. (2) versus time

Transformation time
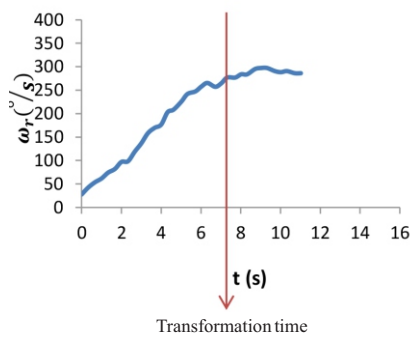
Fig. 15: The values of the omega by Eq. (2) versus time

Transformation time
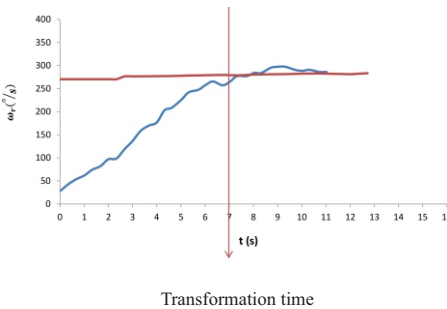
Fig. 16: Comparison the values of the alpha by Eq. (2) and real values from experiments

As it is observed the trend line of the theory fits the actual data for the rotational velocity and this validates equation (1).

Transformation time is an implicitly chosen point to determine transformation from accelerating to rolling state. It is chosen by finding the first point after which omega becomes constant.

We take the values for alpha and omega from the two plots and calculate $\omega_r \, tg \, \alpha$ then plug it into equation (3) and compare the values (Fig. 17).

Fig. 17: Comparison yield that the theory perfectly predicts the velocity trend. Equations are supposed to work in the rolling state.

Equation (6) is a differential equation. We tried to solve this but this equation doesn't seem to have an explicit solution. So computer algorithm was used to draw the explicit plot of alpha per time for each specific case. Figure (18) is an example.

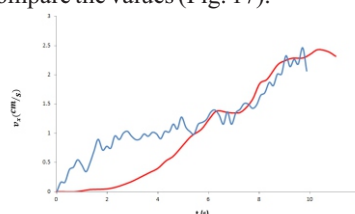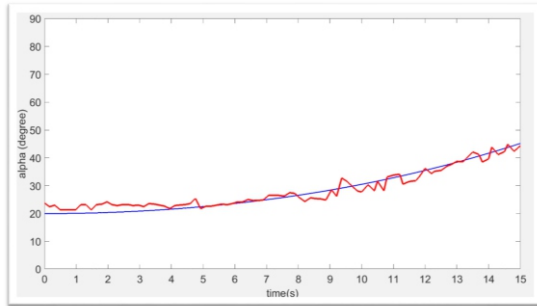**Fig. 18:** Again the theory matches the experimental data and this validates equation (6)

5 Conclusion

The reasons, and the frequently observed cases were investigated in this phenomenon .It is concluded that the horizontal movement of the ring is intrinsic of the circular shapes and the angle between the ring and the shaft. This problem is dividable into two states, the Rolling and Accelerating states. The ring has three Degrees of freedom: Alpha (α) , Omega (ω) and linear velocity (v_x). Each of these attributes can be calculated by the equations (6), (3) and (2), respectively. The more the side thickness of the ring, The more the error. The better the quality of lubrication, the smoother, better and more accurate our results. Air resistance doesn't have a significant effect on the movement, it just causes looping through rolling and accelerating states.

References

[1]   Keith R. S. , 1971. "Mechanics, Massachusetts." .

[2]   Halliday D., Resnick R. and Walker J., 2013. Fundamentals of physics. John Wiley & Sons.

[3]   Innes, G. E., Dowson D. , and Taylor C. M., 1999. "A loose-ring lubricator model." Proceedings of the Institution of Mechanical Engineers, Part C: Journal of Mechanical Engineering Science213.3 : 199-209.

[4]   Simon B., Hawa J., and Salerno J., 2014. "Factors Affecting Oil Ring And Slinger Lubricant Delivery & Stability" Proceedings of the 30th International Pump Users Symposium. Turbomachinery Laboratories, Texas A&M Engineering Experiment Station.

MAKING QUARK

Maysa Naderi [a], Kiana Kamali Poorshiraz [b] , Moujan Naderi Moshaei [c] , MohammadJavad Jafarzadeh [d] , a,b and c) Farzanegan 2 School, Tehran, d) Arman Institute,Mashhad, Iran

A R T I C L E   I N F O

A B S T R A C T

Quark cottage cheese and similar varieties of white acid-set cheese can be produced from milk. In this research as one of the International Young Naturalists' Tournament, IYNT 2018 problems, this process has been investigated experimentally and the properties of the resulting product were studied too.

1 Introduction

According to the main approach : observation, experiment, comparing data and conclusion we are going to investigate this problem.

Cheese as a food derived from milk is produced in a wide range of flavors textures and forms by coagulation of the milk protein casein. During production the milk is usually acidified and adding the enzyme rennet causes coagulation.

Eating high- fat cheese can help to improve our health by raising the high density lipoprotein (HDL) . Low fat cheese has a lower fat which contains at least 25% less fat than its regular counterpart .

Quark Cheese as a traditional creamy cheese is common and popular in German-speaking & Eastern European countries which is often translated to cottage cheese and junket but it is unknown in Asian countries. The traditional one is made without rennet.

2 Experiments

Quark cheese as it was seen under microscope has not a porous texture (Fig. 1).
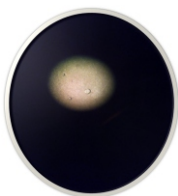

Fig. 1: Quark Cheese under microscope

The recipe to make quark cheese:
4 cups milk , 1/2 teaspoons yoghurt , 1/4 rennet
. Boil the milk on the pan till it had a skin on it
. Let the milk cool to room temperature
. Add the yoghurt
. Stir them & wait they rest at room temperature for 6 hours
. Add the solved rennet
. Stir them in a separated barrel
. Wait for 4 hours
. Layer a strainer with a cotton towel and allow it drains for 7 hours (Fig. 2) .

Fig. 2: Quark cheese is made in our experiment

3 Results

In comparison with other cheese we found its thickness under several weights (Fig. 3).
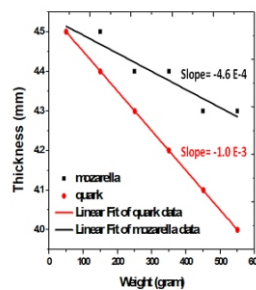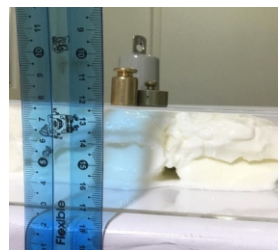
Fig. 3: Comparison between Quark cheese and Mozzarella cheese

Quark contains dramatically less salt than cottage cheese and Ricotta and it has high protein also . Full – fat quark is a great source of vitamin K_2 which helps to maintain bone strength and protect our arteries from block ages . So in the long term consumption it does not make any problem .

Cultures for cheese making are called lactic acid bacteria (LAB) because their primary source of energy is the

lactose in milk and their primary metabolic product is lactic acid that there is a wide variety of bacterial cultures available distinct flavor.

4 Conclusion

Quark is a creamy cheese so it doesn't have a porous texture. It has more benefits than other cheese. Per 100 grams quark contains :

protein 14.1 gr
Sugar 3.5 gr
fat 10.6 gr
saturated fat 7 gr
sodium 81 mg
Energy 690 KJ
calcium 100-130 mg

References

[1]   www.dietvsdisease.org
[2]   www.cheftayebeh.ir
[3]   www.thespruce.com

ALL ROADS LEAD TO ROME

Kiana Kamali Poorshiraz[a], Moujan Naderi Moshaei [b] , MohammadJavad Jafarzadeh[c] , Maysa Naderi[d] , a,b and d) Farzanegan 2 School, Tehran, c) Arman Institute,Mashhad, Iran,

A B S T R A C T

Open a random Wikipedia article and click on the first link in the article. Keep clicking on the first link of each following article. It is argued that you will quickly end up on the page Philosophy. This is one of the IYNT 2018 problems which is investigated whether this is true and how we can describe such an observation.

A R T I C L E   I N F O

1 Introduction

Wikipedia is a free encyclopedia, written collaboratively by the people who use it. It is a special type of website designed to make collaboration easy, called a wiki. Many people are constantly improving Wikipedia, making thousands of changes per hour. All of these changes are recorded in article histories and recent changes.

This research is done by finding random words or random article in Wikipedia and asking questions from different people.

2 Methods

PHILOSOPHY is the study of general and fundamental problems concerning matters such as existence, knowledge, values, reason , mind, and language. By :
- Clicking on the first blue links
- Ignoring external links, links to the current page, or red links.
- Stopping when reaching "Philosophy".

the random word explanation is selected. In this way actually I go to a website which gives us a random word , noun , name , verb and something like this and then I search that word in Wikipedia and saw the result of that .92% of this way ended with the philosophy page but what about the other searches ?

Actually the other searches lead to some pages without any outgoing wiki links or to pages that do not exist that we call it error or maybe sometime get stuck in loops (Fig.1).
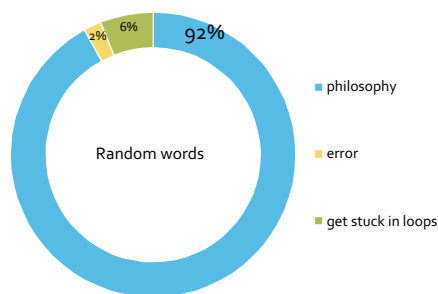
Fig. 1: The result in finding random word

2-1 Random article in Wikipedia

In this way I opened the Wikipedia and Click on Random article and then Wikipedia opened a random article . 96% of my searches in this way ended with the philosophy page (Fig. 2).
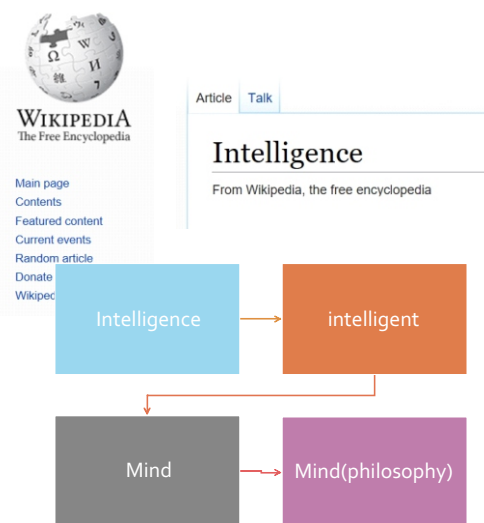
Fig. 2: A random article in wikipedia

2-2 Asking people

In this way I asked people about some random words and after that I searched them in Wikipedia which ended up with philosophy in 79% (Figures 2 and 3).

Fig. 3: The result in asking people

Now I want to sort these searches to some groups and see how many percent of each group end with philosophy (Fig. 4).
My groups:
- Science
- Famous people
- Animals
- Colors
- Location
- Numbers
- Foods and drinks

Fig. 4: Percentage in each groups

In this part if your word was about science you have a chance to end up it in 93% . Fo famous people , 74% it could end up on philosophy page (Fig.5).
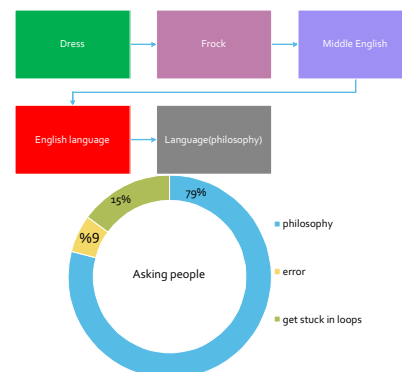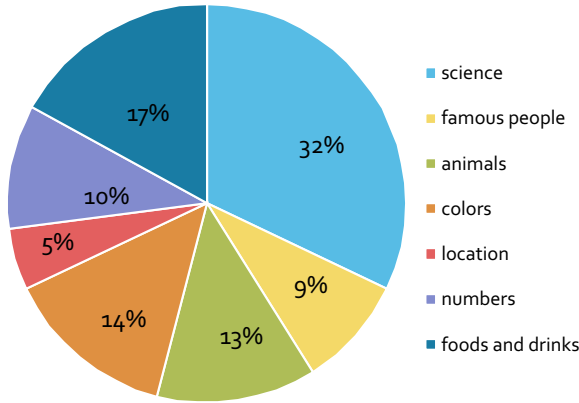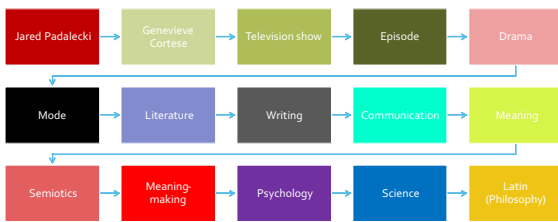

Fig. 5: Famous people searching in wikipedia

If you start with animals you can end up with philosophy in 80% (Fig. 6).
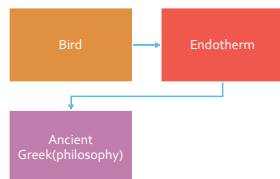
Fig. 6: Searching bird in wikipedia

Finding a location on Wikipedia will end up with philosophy in 93% (Fig.7).
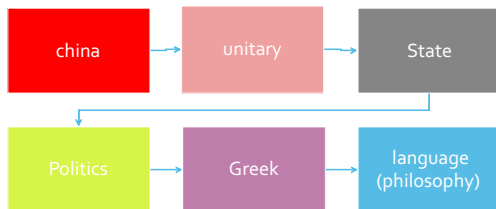
Fig. 7: Searching a location in wikipedia

The colors (blue , gray , red , purple , ….) end up with philosophy in 91% (Fig. 8).
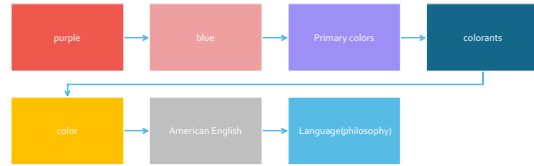
Fig. 8: Colors searching in wikipedia

A number in 97% ,and foods and drinks in 88% .

3 Conclusion

The percentages in whole parts are shown as figure (9).
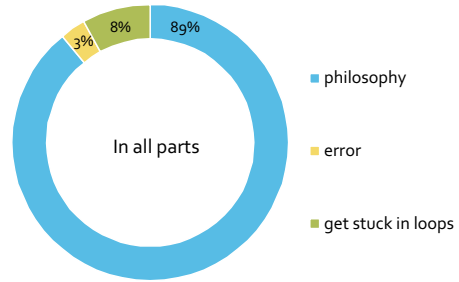
Fig. 9: Total searching in wikipedia

Some theories are performed on this phenomenon, with the most prevalent being the tendency for Wikipedia pages to move up a "classification chain." According to this theory, the Wikipedia Manual of Style guidelines on how to write the lead section of an article recommend that the article should start by defining the topic of the article, so that the first link of each page will naturally take the reader into a broader subject, eventually ending in wide-reaching pages such as Mathematics, Science, Language, and of course, Philosophy, nicknamed the "mother of all sciences" (Figures 10 and 11).
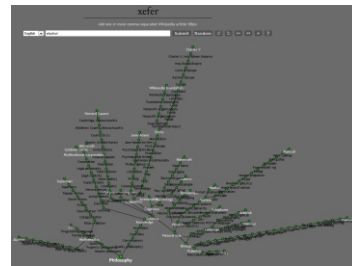
Fig.10: Real classification chain in Wikipedia
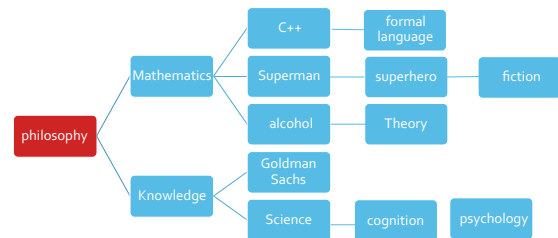
Fig.11: My schematic classification chain for Wikipedia

References

[1]   https://en.wikipedia.org/wiki/wikipedia:Getting to philosophy

Designing an Auxiliary Software to Interpret the Screening of Apoptotic Effect of Drug Compounds by Using AO-EB Test

Darya[a] Talebzadeh, Kiana Mousazadeh [b], a and b) Farzanegan 1 High School, Tehran/ Iran, daryatalebzadeh@yahoo.com

ABSTRACT

In order to solve the problem of counting apoptotic cells stained by AO-EB test, an auxiliary software which can count alive , early apoptosis and late apoptosis cells are designed.

1 Introduction

There are two different types of cell death necrosis and apoptosis. Necrosis happens because of an extrinsic factor and after the cell is in necrosis process the embryonic layer of cell will be inflame and then the cell will die .

The other type of cell death is apoptosis which is a programmed death of cells. Apoptosis can happen both naturally like death of cells which make the membrane between embryos' fingers or can happen by adding drug compounds [1].

Apoptos is a Greek word that means autumn , as autumn doesn't have a bad effect on trees , apoptosis process won't hurt the organism unless we use drug compounds in a wrong way [1].

Both negative and positive effects of apoptosis are possible in different disease.

In one and by chemotherapy extra cancerous cells will be in apoptosis process and die by adding drug compounds, on the other hand apoptosis process needs to be stop in some diseases like Parkinson or heart attack[1,2].

As mentioned the effect of apoptosis process matters and patients must use the right drug to be treated. There are different ways to check the effect of drug compounds on cells, one of the most frequent ways is to stain cells by fluorescence colours like DAPI, HOUKHEST, AO-EB and a specialist count them[2,3].

AO-EB colour is a mixture of both AO and EB colours. All cells absorb AO which is vital stain while EtBr is only absorbed by cells with disrupted membrane (cells in early and late apoptosis state). Alive cells which only absorbed AO will have dark green colour, and cells which absorb both stains (apoptotic cells) become light green (early) and orange-red (late)[4,5].

But the question is that what is the need of this software? Today there are two main ways to check and count the number of cells , one is counting cells by high-tech but too expensive machines like cell machines which are not enough to be used for normal people in some developing countries .

The other way is that specialist count cells . They are able to categorize and count dark and light green apoptotic cells stained by AO-EB. Surely in this way some eye – errors might happen and the accuracy will be low. This software almost solve these problems.

2 Method

Finding the spectrum of red, light and dark green was the first step to analyse pictures. Every digital screen is made by pixels and each pixel has three components R(red), G(green), B(blue) and the measurement of each varies from 0 to 255. Three numbers for each component make the colour of pixels. By these numbers the spectrum are found and then defined to the software.

First of all to analyse one picture the software produce three same sizes of black pictures as the original one for each level of apoptosis. Second pixels which are in one of the defined spectrum in the original picture turn to white in one of the produced black pictures. This process repeats three times in three levels of apoptotic cells and at the end there are three black white pictures that have some errors and mistakes and because the software count the white parts they're not ready to be counted.

To solve mistakes that happen in all image processing programs, four morphology were used ,imdilate , imerode , imopen and imclose. There were some options we had to choose for each morphology. The disk diagram was chosen as a result of cells' shape and then we had to choose a number as the size of filters of each morphology. This morphology has effect on the white parts of black white pictures.

Imdilate makes all white parts thicker ,imerode makes them thinner , imopen deletes all white dots (noises) in the black side of the picture and imclose fills black dots in the white part of the picture.

The first problem was the similarity between dark and light green spectrum and as an example there were some dots in dark green cells (alive) that were in light green (early apoptosis) spectrum so imclose was used to fill the blanks .

Second problem was decomposed cells which were red and didn't have to be counted as a cell and also pixels around light green cells were in light green spectrum so we used imdilate for extra parts to become smaller and in the next step , using imopen made them totally disappear.

At the end there were some cells which weren't fixed and they separated in two or more parts so the last step was using imdilate and all white parts became thicker so separated parts were connected .

After using this morphology, the final picture is complete and also ready to be counted(Figures 1-6).
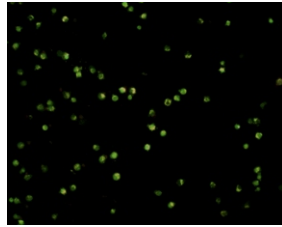

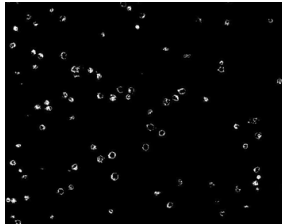**Fig. 1:** Main picture(captured by microscope)

Fig. 2: First step dark green pixels recognition

Fig. 3: Second step imclose morphology

Fig. 4: Third steps imerode morphology

Fig. 5: Fourth step imopen morphology

Fig. 6: Final step imdilate morphology

3 Results

The software starts to analyse pixels from top left of the picture , it analyses pixels one after another in a line. If it is a black pixel nothing happens but for a white one as it's the first white pixel, it counts it as a cell and turns it into black. Then software by checking eight connected pixels to it, turns the white ones into black without counting them. This process repeats three times for all levels.

This way all cells will be counted and the software shows the final result by the percentages of the number of alive, early apoptosis and late apoptosis cells in a pie chart. In order to check the accuracy of the software ,the result of software were compared with the number of cells counted in some authentic articles (tables 1-4) and (Figures 7-10).

Table 1: The comparison [6] of the results for code No751a

Type of cells	The real affluence	Software's affluence
alive	55%	55.3%
early apoptosis	45%	44.7%
Late apoptosis	0%	0%

Fig. 7: Picture of code No751a

Table 2: The comparison [6] of the results for code No533a

Type of cells	The real affluence	Software's affluence
alive	78%	68%
early apoptosis	18%	28.5%
Late apoptosis	4%	3.5%

Fig. 8: Picture of code No 533a

Table 3: The comparison [6] of the results for code No1143a

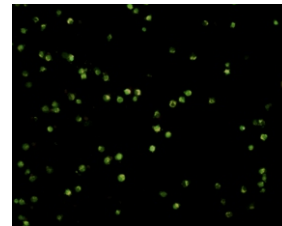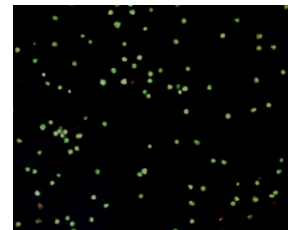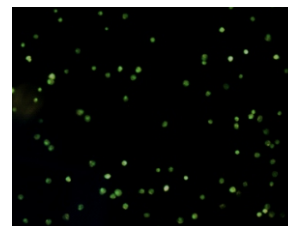| Type of cells	The real affluence	Software's affluence
alive	34%	27%
early apoptosis	62%	73%
Late apoptosis	4%	0%

Fig. 9: Picture of code No1143a

Table 4: The comparison [6] of the results for code No22 43a

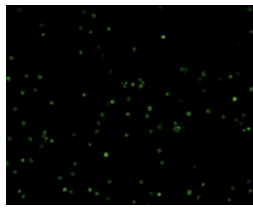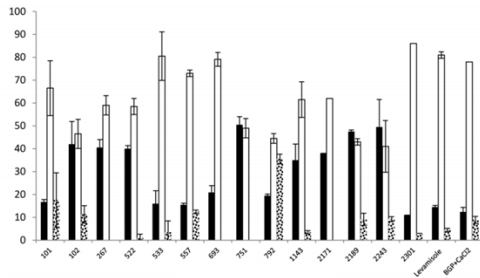| Type of cells	The real affluence	Software's affluence
alive	65%	10%
early apoptosis	28%	90%
Late apoptosis	7%	0%

Fig. 10: Picture of code No 2243a

4 Conclusion

In this new case a different colour range is found, so a new mode can be defined for DAPI staining. In this mode the majority of the pixels are in blue colour range but the detection progress is not far different. First all pixels of the image are classified in two categories, Black and Blue. Then morphological filters are used on the result to remove unwanted cells. This is done by dilating all of the cells. Finally a counting phase will be performed. Since this designated program showed good result in interpretation of AO-EB test result, this program is developed for analysing. The results of staining in determining apoptotic state of treated cells, are the same as DAPI staining which can show apoptotic characteristic of apoptotic cells such as chromatin condensation and DNA fragmentation (Figures 11 and 12) [7,8].

Fig. 11: UTMC codes of the strains

Fig. 12: Comparing different codes

References

[1]   Renvoize, C, Biola, A, Pallardy, M, & Breard, J. ,1998. Apoptosis: identification of dying cells. Cell biology and toxicology, 14(2), 111-120.

[2]   Ribble, D., Goldstein, N.B., Norris, D.A. and Shellman, Y.G., 2005. A simple technique for quantifying apoptosis in 96-well plates. BMC biotechnology, 5(1), p.12.

[3]   Prem Kumar V. et al., 2011. Object counting and density calculation usingmatlab,computer science,4,44-52.

[4]   Ma, Y., Zhang, G. and Pan, J., 2012. Spectroscopic studies of DNA interactions with food colorant indigo carmine with the use of ethidium bromide as a fluorescence probe. Journal of agricultural and food.

[5]   Zhang, H., Zhao, X., Liu, S., Yang, J., Duan, R., Yuan, Y. and Hu, X., 2017. Determination of Sunset Yellow Based on Its Quenching Effect on the Fluorescence of Acridine Orange.Analytical Sciences, 33(2), pp.243-247.

[6]   Salimi F, Hamedi J, Motevaseli E, Mohammdipanah F., 2017. Isolation and screening of rare Actinobacteria, a new insight for finding natural products with antivascular calcification activity, journal of applied microbiology.

[7]   Friedrich O.,1990. "DAPI staining of fixed cells for high-resolution flow cytometry of nuclear DNA." Methods in cell biology. Vol. 33. Academic Press, 105-110.

[8]   Bron D. and DeCoster A.D., 2004. "Quantification of sPLA2-induced early and late changes in neuronal cell cultures using combined TUNEL and DAPI staining." Brain Research Protocols 13.3 144-150.

INVESTIGATING A PNEUMATIC HORN

Aida Doostmohammadi, Absal Smart High School, Tehran/ Iran, aida.dm2013@yahoo.com

A B S T R A C T

A simple air horn can be constructed by stretching a balloon over the opening of a small container or cup with a tube through the other end. Blowing through a small hole in the side of the container can produce a sound. The relevant parameters which affect the sound have been investigated in this research as one of the problems in IYPT 2017.

A R T I C L E   I N F O

1 Introduction

An air horn is a pneumatic device designed to create an extremely loud noise for signaling purposes. Air horns are widely employed as vehicle horns, installed on large semitrailer trucks, fire trucks, trains, and some ambulances as a warning device and on ships as a signaling device. An air horn consists of a flaring metal or plastic horn or trumpet attached to a small air chamber containing a metal pipe or diaphragm in the throat of the horn.

Compressed air flows from an inlet line through a narrow opening past the pipe or diaphragm, causing it to vibrate, which creates sound waves. The flaring horn serves as an acoustic "transformer" to improve the transfer of sound energy from the diaphragm to the open air, making the sound louder. In most horns it also determines the pitch of the sound. There are different types of acoustic pipes, open ended pipe or closed ended pipe. In this problem we need to use open ended pipe it means if the sides of the pipe are open.
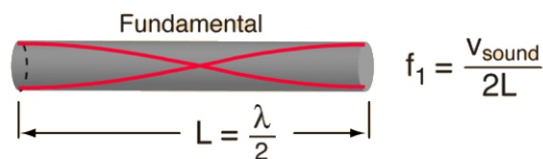

Fig.1: Standing waves in open ended pipe

2 Theory and Modeling

This phenomenon occurs when we blow to the air horn then a certain amount of air goes into the bottle. Normally, a given volume of air inside the bottle has the temperature and pressure same as outside the bottle[1]. But when you blow to the air horn , the pressure inside the bottle becomes more than the pressure outside but here it is investigated as an ideal gas, $PV=nRT$.

Sound is a longitudinal wave that the direction of propagation is parallel to the direction of vibration. When a person blows to this air horn balloon, the balloon starts getting up and the inducement is that the high pressure area enters it and because of keeping out of the pipe, the internal pressure reduces. Therefore, it connected to the container again (Fig. 2) [2].
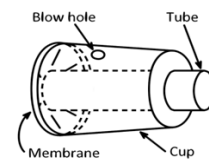

Fig. 2: Experimental Airhorn Balloon structure

2-1 Voice pipe

The quality in a sound of being deep is called resonance. When the inherent frequency of voice pipe resonance with frequency wave , it creates better sound. (When the inherent frequency becomes as same as the frequency wave).One of the most important parameters is voice pipe because it has a dramatic effect on the sounds and frequency. Different diameters and pipe length are also important factors in a distinct frequency.

2-2 Membrane (Balloon)

The membrane has a dramatic effect on the sound too. Elasticity, thickness and also material of the membrane are considered as important factors in experiments and results.

2-3 Hole

The size of the hole has much effect on sound. When the hole is small, the person has to blow into it strongly. But when it is bigger the sound will spread easily.

3 Experiments

By different sizes of airhorn (Fig. 3) , all the produced sounds are analyzed by FFT (Fast Fourier transform analysis) which converts a signal from its original domain (often time or space) to a representation in the frequency domain and vice versa.

Fig. 3: Different sizes of Airhorn Balloon in our experiment

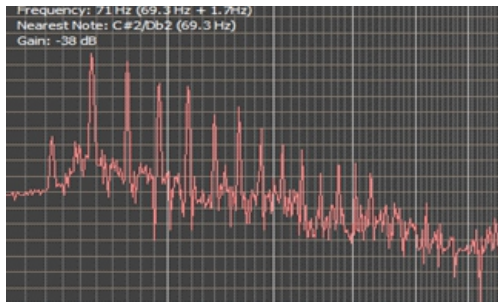FFT analysis and natural frequencies of the cup are shown in figures (4 and 5).

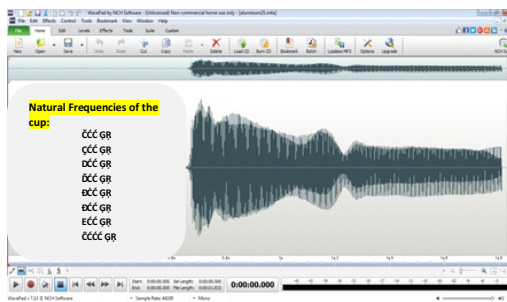

Fig. 4: FFT analysis in air horn [3]

Fig. 5: Wave Pad Sound Editor application

4 Results

Tubes with different lengths and materials are used to find the frequency as in tables (1 and 2).

Table 1: Changes of frequency in different lengths and materials of airhorn

Tube Size and Material	Frequency
20 cm aluminum	678(Hz)
50 cm aluminum	270(Hz)
20 cm Galvanized	425(Hz)
30 cm Galvanized	406(Hz)
40 cm Galvanized	309(Hz)
50 cm Galvanized	265(Hz)
18 cm plastic	506(Hz)
21 cm plastic	431(Hz)

Different materials of cup are considered in this experiment too (table 2).

Table 2: Changes of frequency in different lengths and materials of airhorn

Cup Size and material	Frequency
15 Cm Plastic	130 Hz
15 Cm Aluminium	120 Hz
18 Cm Plastic	200 Hz

5 Conclusion

Different parameters like the shape, size and material of the components have been investigated. Membrane has an important effect on the sounds in airhorn with the significant impact by its elasticity, thickness and also material. If the traction of balloon becomes further, the voice becomes thinner and vice versa. Also by different tubes, it is suggested a tube with effective length for the best sound.

References

[1]   Bobby Mercer., 2014.”50 Awesome Experiments That Don't Cost a Thing.”(Chicago Review Press, 2014) Junk Drawer Physics:73-77, https://books.google.com/books?id=3eWLAwAAQBAJ

[2]   Billah KY., and Scanlan RH., 1991.”Resonance, Tacoma Narrows bridge failure, and undergraduate physics textbooks.” American Journal of Physics: 59, 118 , math.arizona.edu

[3]   NTCH software.,”WavePad Sound Editor application”, https://wavepad.en.softonic.com/

Ariaian Young Innovative Minds Institute, AYIMI
Unit 14, No. 32, Malek Ave., Shariati St.
Post Code: 1565843537
Tel - Fax: +9821-77522395, 77507013
Tehran/ Iran
URL: http://www.ayimi.org
        http://journal.ayimi.org
Email: info@ayimi.org